CALCIUM DYNAMICS OF GANGLION CELL LAYER NEURONS IN *RD1* MICE

by

Jessica Anita Carr

Submitted in partial fulfillment of the requirements
for the degree Master of Science

at

Dalhousie University
Halifax, Nova Scotia
June 2020

Dedication

To Mum and Dad.

Thank you for inspiring me everyday to be kind and work hard,

to believe in myself,

and to strive to do my best.

Love you tons

Table of Contents

List of Tables

List of Figures

Abstract

In the *rd1* mouse model of inherited retinal degeneration, activation of P2X7 purinoreceptors (P2X7r) has been suggested to lead to the formation of pores permeable to large molecules in retinal ganglion cells (RGCs). This suggests that retinal neurons downstream from degenerating photoreceptors are also affected during retinal degeneration, a phenomenon that could limit the effectiveness of treatment modalities for vision restoration that replace or restore photoreceptor function alone. P2X7r pores could increase intracellular calcium concentration ($[Ca^{2+}]_i$) and possibly cause cell death, but RGC calcium dynamics in the *rd1* mouse have not been studied. The objective of this thesis was to examine Ca^{2+} indicator dye loading and the calcium dynamics (resting $[Ca^{2+}]_i$ and kainic acid (KA)-induced Ca^{2+} response) of ganglion cell layer neurons (GCLn) in *rd1* (C3H/HeJ) mice in comparison with wt (C57BL/6) mice. Freshly enucleated eyes were used and fura-2 loaded into GCLn either by intravitreal injection or applied to isolated retinas. In some cases, eyes were electroporated or P2Xr antagonists applied (A740003, P2X7r antagonist, 10 μM; PPADS, P2r antagonist, 1 mM; TNP-ATP, P2Xr antagonist, 500 μM). The fura-2-loading was compared with loading of the known P2X7r-permeable dye YO-PRO-1 (100 nM) in *rd1* GCLn. Fura-2-loaded retinas were superfused with oxygenated Hank's solution and fura-2 ratiometric calcium imaging of GCLn performed. To assess GCLn calcium dynamics, the resting $[Ca^{2+}]_i$ was recorded and KA (AMPAr agonist, 50 μM) was superfused to evoke transient increases of fura-2 ratio (indicating an increase of $[Ca^{2+}]_i$). Purinergic drugs (A740003, P2X7r antagonist, 10 μM; apyrase, ATP-degrading enzyme, 5 units/ml; BzATP, P2X7r agonist, 250 μM; ATPγS, P2 agonist, 185 μM) were applied to assess the influence of the purinergic signalling pathway on resting $[Ca^{2+}]_i$ and on KA-induced Ca^{2+} responses. In *rd1* retinas, fura-2 loaded GCLn without the need for electroporation; however, loading was not reduced with P2Xr antagonists and fura-2 did not load the same population of GCLn as YO-PRO-1. Baseline $[Ca^{2+}]_i$ was similar in GCLn in *rd1* and wt retinas and purinergic drugs application had no effect. The KA-induced Ca^{2+} response was significantly greater in *rd1* GCLn than wt GCLn. The enhanced response was blocked by P2X7r antagonist (A740003) but recovered by subsequent treatment with ATPγS. There was no effect of purinergic agonists on KA-induced Ca^{2+} responses when applied alone in either *rd1* or wt GCLn. These results suggest that the enhanced KA-induced Ca^{2+} response in *rd1* GCLn depends on P2X7r but does not involve ATP acting on P2X7r. A possible model is that P2X7r on other cell types in the retina release ATP through P2X7r pores and this ATP then affects the fura-2-loaded GCLn either directly, or indirectly, by acting on other P2r. Broadly, these data suggest that there is altered purinergic signalling in the *rd1* retina, adding to the growing evidence that retinal neuron types other than photoreceptors are affected during retinal degeneration.

List of Abbreviations Used

$[Ca^{2+}]$	Calcium concentration
$[Ca^{2+}]_i$	Intracellular calcium concentration
A74	A740003
A740003	*N*-(1-[[(Cyanoamino)(5-quinolinylamino)methylene]amino]-2,2-dimethylpropyl)-3,4-dimethoxybenzeneacetamide
ADP	Adenosine diphosphate
AMPA	α-amino-3-hydroxy-5-methyl-4-isoxazolepropionic acid
Apyr	Apyrase
ATP	Adenosine triphosphate
ATPγS	Adenosine-5'-(γ-thio)-triotriphosphate tetralithium salt
au	Arbitrary unit
BBG	Brilliant blue
BzATP	2'(3')-*O*-(4-Benzoylbenzoyl)adenosine 5'-triphosphate triethylammonium salt
Ca^{2+}	Calcium
CNS	Central nervous system
cGMP	Cyclic guanosine monophosphate
DNA	Deoxyribonuclaic acid
DMSO	Dimethyl sulfoxide
e^-	Electroporation
ERG	Electroretinogram
FOV	Field of view
Fura-2 $5K^+$	Fura-2 pentapotassium salt
GCL	Ganglion cell layer
GCLn	Ganglion cell layer neurons
HBS	Hank's balanced salts
HBSS	Hank's balanced salts solution
HEPES	4-(2-hydroxyethyl)-1-piperazineethanesulfonic acid
INL	Inner nuclear layer
IPL	inner plexiform layer
ipRGC	Intrinsic photosensitive retinal ganglion cell
KA	Kainic acid
LGN	Lateral geniculate nucleus
mGluRs	Metabotropic glutamate receptors
Na^+	Sodium
NaOH	Sodium hydroxide
NMDA	*N*-methyl-D-aspartate
ONFL	Optic nerve fiber layer
ONL	Outer nuclear layer
OPL	Outer plexiform layer
P2r	P2 receptor family
P2X7r	P2X7 receptor
P2Xr	P2X receptor family

PCR	Polymerase chain reaction
PDE	Phosphodiesterase
PPADS	Pyridoxalphosphate-6-azeophenyl-2'-4'-disulfonic acid tetrasodium salt
PRL	Photoreceptor layer
RBPMS	RNA-binding protein with multiple splicing
RGC	Retinal ganglion cell
ROI	Region of interest
RP	Retinitis pigmentosa
RPE	Retinal pigmented epithelium
SD	Standard deviation
TNP-ATP	2'-3'-*O*-(2,4,6-Trinitrophenyl)adenosine-5'-triphosphate tetra(triethylammonium) salt
TRPV1	Transient receptor potential vanilloid type-1
UDP	Uridine diphosphate
UTP	Uridine triphosphate
V1	Primary visual cortex
VGCC	Voltage-gated calcium channel
wt	Wildtype

Acknowledgements

My sincerest gratitude goes to my supervisor, **Dr. Bill Baldridge**, for the continued support during my MSc studies and research. Thank you for the guidance and all the opportunities you have provided me with. I am so lucky to learn from you and could not have imagined having a better mentor.

To my committee **Dr. François Tremblay**, **Dr. Spring Farrell**, and **Stephanie Smith**; thank you all for your continued support, time, and kindness. Your expertise is awe-inspiring, and I have learned so much from you all. Thank you to **Margaret Luke** for providing the wildtype ERG data.

To the **IWK orthoptics teachers** who became coworkers, the **CVS grads and current students** who love everything eye-related as much as I do, my **LASIK team** who have became best friends, and my wonderful **colleagues in the Retina and Optic Nerve Research Lab**: thank you for providing a fantastic support system here in Halifax. I love that I had the opportunity to be part of so many amazing positive communities. The thank you list is so long that I could write an entire novel of thank you's that still would not do you all justice – I am so grateful.

To my brother **James Carr**, thank you for teaching me that even thought roadblocks happen and things can be tough there is always a bright side and we can come out stronger than ever. Thank you for always finding something to tease me about (as much as I protest), keeping me laughing, and for your radiating positivity.

To my aunt **Jen Hatto**, thank you for the getaway trips to Moncton, the animal therapy and your delicious meals and laughs. You are absolutely amazing.

And to my fur baby, **Poppy**. Meow, meow, meow, purr, purr, purr.

The last four year spent in beautiful Halifax have been outstanding; to everyone who I have met and supported me in my studies- Thank you.

Chapter 1: Introduction

1.1: The Eye and Retina

They eye has numerous components, each with an essential role for vision. Light enters the eye by passing through the tear film and the cornea (the transparent avascular external surface of the eye) where it is refracted and passes through the aqueous humour and the pupil of the iris. The lens is the second location where refraction occurs, and light then travels through the vitreous to reach the retina on the inner surface of the posterior globe. The retina converts the photons that constitute the visual image into an electrochemical signal and processes this signal before delivering it to the brain via the optic nerve. Although several brain regions in humans receive projections from the retina, for visual perception the relevant target is the lateral geniculate nucleus (LGN) of the thalamus. Optic radiations project from the LGN to terminate in the primary visual cortex (V1) of the cerebrum. The visual signal is then further processed by higher cortical regions. (Van Essen *et al*. 1992, Sanes and Zipursky 2010, Remington 2012)

The neural retina is a transparent piece of central nervous tissue composed of neurons and glia organized into histologically visible stratified layers defined by different cell types or synaptic junctions. Broadly, the signal pathways in the retina can be classified as being either vertical or horizontal. The vertical pathway involves synaptic connections between photoreceptors and bipolar cells, and between bipolar cells and ganglion cells. The vertical path is modulated by the horizontal pathway, namely horizontal cells and amacrine cells. Glial cells in the retina include Müller cells,

microglia, and astrocytes. The basic structural organization of the retina is conserved across the vertebrates (Sanes and Zipursky 2010).

The retina is divided into three cellular layers interposed by two synaptic or plexiform layers. The outermost layer consists of the outer and inner segments of photoreceptors, located in the photoreceptor layer (PRL), and outer nuclear layer (ONL), respectively. The outer segments of the PRL contain photopigment (see below) and the inner segments contain the photoreceptor metabolic organelles and is the location of the photopigment production. The ONL is made of the cell bodies of the photoreceptors. The next layer is the outer plexiform layer (OPL) that contains the synapses between photoreceptor synaptic terminals and the dendrites of second-order neurons, horizontal cells and bipolar cells. The inner nuclear layer (INL) contains the cell bodies of horizontal, bipolar and amacrine cells. The inner plexiform layer (IPL) consists of the synapses formed between bipolar and amacrine cells and ganglion cells. The ganglion cell layer (GCL) consists of both retinal ganglion cells (RGCs) and displaced amacrine cells. The axons of ganglion cells form the optic nerve fiber layer (ONFL) which come together at the posterior pole to form the optic nerve. Müller glia cells span the retina from the ONL to ONFL, forming the outer and inner limiting membranes, and provide structural and metabolic support for the retina (Masland 2001, Bringmann *et al.* 2006, Sanes and Zipursky 2010).

Distal to the neural retina is the retinal pigmented epithelium (RPE) that consists of metabolic support cells for rod and cone photoreceptors. The RPE not only helps photoreceptors meet their great metabolic demand but also is essential for the rod visual cycle produced by the recycling of chromophore (Strauss 2005).

Photoreceptors are the first cells of the visual pathway and convert light into an electrical signal that then modulates the release of the neurotransmitter glutamate onto the dendrites of the second-order neurons, the horizontal and bipolar cells. The process by which photoreceptors convert light energy into an electrical signal is called phototransduction (Stryer 1986). Phototransduction is initiated when light is absorbed by a membrane-bound light-sensitive photopigment molecule in the photoreceptor outer segment. The photopigment is called rhodopsin in rods and opsins (S, M, and L subtypes) in cones. Much of phototransduction was determined by studying rhodopsin, but the general features of cone phototransduction are similar. The photopigment complexes are a combination of rhodopsin or cone opsins and a covalently-bound chromophore, retinaldehyde (retinal, a derivative of dietary vitamin A) (And and Ebry 1986). When rhodopsin absorbs light energy, the chromophore undergoes a photoisomerization event where it changes configuration from 11-*cis*-retinal to all-*trans*-retinal (Arshavsky *et al.* 2002). This configuration causes exposure of an intracellular catalytic site on the opsin protein (which is now called metarhodopsin II) that activates a G-protein called transducin (T_α) by separating the α subunit from the $\beta\gamma$ subunit (Stryer 1986). The T_α binds to and activates cyclic GMP phosphodiesterase (PDE) and this leads to the hydrolysis of cGMP to 5'GMP (Stryer 1986). The lowered level of intracellular cGMP promotes closing of cGMP-gated cation channels (Arshavasky *et al*. 2002, Palczewski 2006). In the dark, photoreceptors are continuously depolarized by cation influx through the cGMP-gated channels and this produces a constant release of the excitatory neurotransmitter glutamate onto the dendrites of horizontal cells and bipolar cells (Hagins

et al. 1970). When the cGMP-gated channels close in response to light, photoreceptors hyperpolarize, which reduces glutamate release (Bloomfield and Dowling 1985).

The synapses that occur in the plexiform layers between the vertical pathway cells (photoreceptors - bipolar cells - ganglion cells) are glutamatergic (Bloomfield and Dowling 1985). However, in the OPL, the synapse location and polarity of signal transmission are different depending on the subtype of bipolar cell. Two signalling pathways emerge at the photoreceptor-bipolar cell synapses: a depolarizing ON pathway and a hyperpolarizing OFF pathway (Ashmore and Copenhagen 1980). As the names suggest, ON bipolar cells depolarize in response to light and OFF bipolar cells hyperpolarize in response to light. The two types of bipolar cell dendrites are anatomically distinct: ON bipolar cell dendrites invaginate within photoreceptor synaptic terminals and OFF bipolar cell dendrites form flat contacts with photoreceptor synaptic terminals (Hopkins and Boycott 1997, Haverkamp *et al.*2000).

The response polarity of each type of bipolar cell is due to the presence of different types of glutamate receptors. There are two classes of glutamate receptors: ionotropic and metabotropic. Ionotropic glutamate receptors are ion-channel-associated receptors that directly gate the passage of ions across cellular membranes (Collingridge and Lester 1989). There are three main subcategories of ionotropic receptor, originally named based on agonists selective for each receptor: NMDA, AMPA, and kainate (Davies and Watkins 1979, McLennan 1983, Bleakman and Lodge 1998). Metabotropic glutamate receptors are G-protein-coupled receptors that initiate intracellular signal transduction cascades that modulate ion channels (Blackshaw *et al.* 2011). ON bipolar cells utilize metabotropic glutamate receptors that produce hyperpolarization in the

presence of glutamate. When glutamate released from photoreceptor is decreased during a flash of light, ON bipolar cell depolarize (sign-inverting synapse). OFF bipolar cells possess ionotropic glutamate receptors that cause depolarization by glutamate (sign-conserving synapse). Therefore, when glutamate release from photoreceptors is decreased during a flash of light, OFF bipolar cell hyperpolarize.

The ON and OFF signal is passed from bipolar cells to RGCs via sign-conserving glutamatergic synapse employing ionotropic glutamate receptors on RGC dendrites (Gao *et al.* 2013). In relation to the responses generated by bipolar cells, the types of RGCs, described first by Hartline in 1938, are ON, OFF, and ON-OFF. The ON and OFF signals from bipolar cells are propagated to the dendrites of corresponding RGCs within the IPL (Boycott *et al.* 1969); ON bipolar cell axons connect to ON RGC dendrites in the inner IPL (sublamina b), OFF bipolar cell axons connect to OFF RGC dendrites in the outer IPL (sublamina a), and both types connect to ON-OFF RGC dendrites that span the entire width of the IPL (Nelson *et al.* 1978, Pang *et al.* 2002). In humans, the vertical pathway RGCs then project to the lateral geniculate nucleus (LGN) of the thalamus.

1.2: Inherited Retinal Degeneration

Inherited retinal degeneration are retinopathies that involve the loss or dysfunction of genes associated with photoreceptor viability or function, including the phototransduction pathway (Duncan *et al*. 2018). These include human diseases that have corresponding animal models such as: retinitis pigmentosa, Leber's congenital amaurosis, Best vitelliform macular dystrophy, Stargardt disease, and age-related macular degeneration. Current strategies to treat and restore vision loss in patients with retinal

degeneration include gene therapy and optogenetics, cell transplantation, and electrical implants (Bakondi *et al.* 2015, Tochitsky *et al.* 2016, Schwartz *et al.* 2015, Zrenner *et al.* 2011). However, the success of these treatments depends on both the viability of the remaining retinal circuitry following photoreceptor degeneration and the stage when treatment is to occur.

There are numerous downstream functional and morphological changes that occur following photoreceptor death that are common among inherited photoreceptor degenerative diseases. Marc *et al*. (2003) have classified these retinal changes into three phases. Phase 1 involves rod degeneration and death that is accompanied with cone outer segment truncation and rod neurite extension into inner retinal layers (Kolb and Gouras 1974, Marc *et al.* 2003, Kalloniatis *et al*. 2016). Phase 2 involves cone degeneration with cone neurite extension and retraction of bipolar and horizontal cell dendrites (Marc *et al.* 2003). Müller cells also become dysfunctional in phase 2; they undergo somatic translocation to the ONL and form a glial fibrotic seal by filling in gaps left by dying photoreceptors in the outer retina (Marc *et al.* 2003, Jones and Marc 2005). Phase 3 involves global neuronal remodeling as the remaining neurons are isolated from excitatory synaptic activity, die and form microneuromas (tangles of processes of amacrine cells, bipolar cells, and RGCs) (Jones and Marc 2005). Extensive retinal rewiring occurs during this phase and horizontal and amacrine cells undergo neurite sprouting to contact many of the remaining cells (Fariss *et al.*2000, Marc *et al.* 2003).

Despite these changes in the outer and inner layers of the retina, RGCs remain present and connected to the brain (Jones and Marc 2005, Margolis *et al*. 2008). The integrity of these RGCs have been widely considered as a possible target for vision-

restoring treatments. In the *rd1* mouse model of retinal degeneration (see Section 1.3), Margolis *et al*. (2008) examined RGC dynamics using patch-clamp recordings and two-photon microscopy. They confirmed findings from multielectrode array experiments by Stasheff (2008) that RGCs had increased oscillatory spontaneous spike activity secondary to retinal remodeling. Margolis *et al.* (2008) also found that some characteristics in RGCs were maintained after photoreceptor degeneration: intrinsic firing properties (excitation-mediated action potential generation), dendritic stratification within in the IPL, and dendritic calcium signalling. In addition to the retinal changes, Saha *et al*. (2016) discovered in the *rd1* mouse model that there is reduced density of excitatory synapses onto ON RGCs and inhibitory synapses onto OFF RGCs. Therefore, RGCs remain present and express some regular characteristics, but are altered during the retinal remodelling process associated with photoreceptor cell death.

1.2.1: Retinitis Pigmentosa

Retinitis pigmentosa (RP) is a family of human inherited retinal degenerations classified by photoreceptor cell death (Hamel 2006). Clinical characteristics of RP include progressive night blindness and peripheral vision loss causing tunnel vision, narrowing of retinal blood vessels, and bone spicules caused by RPE degeneration and migration (Grover *et al.* 1990, Milam *et al.* 1998, Li *et al.* 1995). Signs and symptoms in human RP appear at varying stages of disease progression; night blindness is one of the first (commonly during adolescence), while fundus bone spicules may become apparent in late stages (Milam *et al*. 1998). An important diagnostic tool for RP is the electroretinogram (ERG), which is an electrophysiological test for retinal function.

Studies have consistently demonstrated abnormal light-induced retinal responses in RP with reduced ERG photoreceptor a-wave and bipolar cell b-wave amplitudes (Berson *et al.* 1968, Cideciyan and Jacobson 1993). RP is a rod-cone dystrophy which indicates rods degenerate first followed by cones, and, as an inherited retinal degenerative disease, there is extensive retinal remodelling following photoreceptor cell death (Marc *et al.* 2003). RP has been associated with many genes; it can be caused by autosomal recessive, autosomal dominant, and X-linked non-syndromic inheritance patterns, and is associated with syndromes such as Ushers, Bardet-Biedl syndrome, and neuropathy (Ferrari *et al.* 2011). With many different known genetic etiologies of RP, the vast number affect components of the phototransduction pathway, retinal metabolism, tissue development and maintenance, or photoreceptor structural integrity (Ferrari *et al.* 2011).

1.3: The C3H Mouse

The C3H mouse (also referred to as *rd1*) is an important animal model in research and was originally bred in 1920 by Strong (1935). The C3H mouse model has been used in many different fields of study such as breast cancer research (Heston and Vlahakis 1971, Silverman *et al.* 1989) and research on infectious diseases such as salmonella and endotoxin (Cheers and McKenzie 1978, Eisenstein *et al*. 1982). The C3H strain is homozygous for the retinal degeneration mutation called Pde6b^{rd1}, the same mutation responsible for an autosomal recessive form of RP in humans (Carter-Dawson *et al*. 1978). This mutation renders mice blind and unresponsive to light-evoked activity by wean age (~ post-natal day 20) (Bowes *et al.* 1990, Stasheff 2008). The Pde6b^{rd1} genetic mutation affects the function of the cGMP phosphodiesterase (PDE) enzyme which, as

described in Section 1.1, is expressed in photoreceptors and is an essential enzymatic component in the phototransduction pathway (Bowes *et al.* 1990). The mutation affects the expression of the β subunit of PDE and renders it inactive, causing an accumulation of cGMP in photoreceptors (Bowes *et al.* 1990). The accumulation is believed to cause metabolic dysfunction and the degenerative processes leading to photoreceptor death (Farber and Lolley 1976, Bowes *et al*. 1990). The mutation in mice causes photoreceptor cell death and produces a phenotype in the mice similar to the phenotype of retinitis pigmentosa in humans: progressive blindness, retinal vessel weakening, and bone spicule pigmentation in the fundus (Kalloniatis *et al.* 2016, Grover *et al.* 1990).

1.4: P-Family Receptors

As described above (Section 1.1), glutamate is the principal excitatory neurotransmitter in the retina. Nucleotides and nucleosides, such as ATP and adenosine, are important for cellular metabolism, energy, and the formation of genetic material, and also serve as neurotransmitters or neuromodulators in the central nervous system, including the retina (Drury and Szent-Gyorgyi 1929, Khakh and Burnstock 2009, Idzko *et al.* 2014). ATP and P2X7 purine receptors have been suggested to be altered in the *rd1* mouse model of retinal degeneration (see Section 1.4.2 below, Tochitsky *et al.* 2016).

Extracellular nucleotides and nucleosides target two major families of membrane-bound purinergic receptors called P1 and P2 receptors, respectively, each of which are further subcategorized (Ralevia and Burnstock 1998). P1 receptors are G protein-coupled and activated by adenosine; they consist of 4 subtypes based on molecular, biochemical, and pharmacological variations (Khakh and Burnstock 2009). P2 receptors are activated

by ATP (adenosine triphosphate), ADP (adenosine diphosphate), UTP (uridine triphosphate), and UDP (uridine diphosphate), and are further split into P2Y and P2X receptor families (Ralevia and Burnstock 1998, Coddou *et al.* 2011). The P2Y receptors are G protein-coupled receptors and have 8 subtypes identified in mammalian cells (Fischer and Krügel 2007). The P2X receptors consist of trimeric ligand-gated cation channels, are activated by ATP, and have 7 subtypes identified in mammalian cells (called P2X1-P2X7) (North 2002, Coddou *et al.* 2011).

Each P2X receptor contains an ectodomain (the portion of the protein extending into extracellular space where ligand binding occurs), two transmembrane domains (the portion that spans the plasma membrane), and intracellular N and C terminals (responsible for receptor desensitization and/or pore dilation) (Coddou *et al.* 2011). An additional classification criterion for ion channels is the size of their openings: ion selective channels (permeable to small molecules) and pores (permeable to larger molecules). What is interesting about the P2X receptor family is that the P2X2, P2X4, P2X5 and P2X7 subtypes fall into both ion channel classifications (Virginio *et al.* 1999, Bartlett *et al*. 2014). Under prolonged activation by extracellular ATP, the channels dilate to form a pore in the cellular membrane that allows passage of larger molecules (Rassendren *et al*. 1997). The P2X subcategory is the receptor of interest in the current thesis, specifically the P2X7 receptor (P2X7r).

1.4.1: P2X7 Receptors

Early studies performed on macrophage immune cells expressing the now-known P2X7r revealed that high concentrations of extracellular ATP caused cells to uptake dye,

release proinflammatory mediators, and undergo cytolysis and death (Steinberg *et al.* 1987, Zambon *et al*. 1994, Di Virgilio 1995). Before 1996, it was believed there were only 6 subtypes of P2X receptors and another receptor, called the P2Zr, was located on immune cells and responsible for the macrophage findings by Steinberg *et al.* (1987). However, in 1996, Surprenant *et al.* isolated complementary DNA for a P2X receptor that coded for an amino acid sequences different from any known P2X receptors. They found that the mRNA for this receptor was strongly expressed in the same macrophage cells and determined that the original P2Zr in the macrophage studies was in fact a seventh member of the P2Xr family (P2X7). Since the discovery in macrophages, the P2X7r has been identified in many different parts of the body: immune cells, blood cells, bones, endothelial and epithelial cells, fibroblasts, and the nervous system including neurons, glia and astrocytes (Burnstock and Knight 2004, Bartlett *et al.* 2014).

The P2X7r is a homomeric and trimeric, ATP-gated cation transmembrane channel (Surprenant *et al.* 1996, Jiang *et al.* 2013). As mentioned above, when ATP binds to P2X7r, the ion channel opens to allow the passage of small cations (Ca^{2+}, Na^{+}, and K^{+}) and, under prolonged activation with extracellular ATP, dilates into a large conductance channel (pore) (Rassendren *et al*. 1997). Steinberg *et al.* (1987) were one of the first to use fluorescent dyes to functionally evaluate ATP-induced cell loading through the now-known P2X7r pore. They found that extracellular ATP caused loading with dyes in the 376-831 Da molecular weight range (6-carbozyfluorescein, 376 Da; lucifer yellow, 457 Da; fura-2, 831 Da) but not 961 Da or larger (trypan blue, 961 Da; Evans blue, 961 Da). It is now understood that the P2X7 receptor allows the passage of molecules up to ~900 Da in size (Surprenant *et al.* 1996, Yan *et al.* 2008).

Extracellular ATP is degraded and kept at low concentration by ectonucleotidases (enzymes which metabolize ATP) at synaptic terminals (Puthussery *et al*. 2006). Lenertz *et al*. (2011) proposed that P2X7r pores are only activated in situations with pronounced elevation of extracellular ATP such as infection, injury, or in tumours. The P2X7r has also been called the "death receptor" due to its role in mediating cell apoptosis and the activation of caspases (Ferrari *et al.* 1999). In some situations, activation of the P2X7r by extracellular ATP stimulates further ATP release through the receptor, for example in osteoclasts during fusion and maturation (Pellegati *et al.* 2011) and in melanoma cells after γ-irradiation (Ohshima *et al*. 2010).

In the retina, the P2X7r is expressed by many cell populations including photoreceptors, amacrine cells, RGCs and Müller cells (Brändle *et al.* 1998, Pannicke *et al.* 2000, Wheeler-Schilling *et al.* 2001, Puthussery and Fletcher 2006). There have been several studies that examined the harmful effects of P2X7r activation in the retina. Puthussery and Fletcher (2009) found that intravitreal injections of ATP caused photoreceptor apoptosis in rat retina. Similarly, Notomi *et al*. (2011) found that intraocular injection of the P2X7r agonist BzATP, (2'(3')-*O*-(4-Benzoylbenzoyl)adenosine 5'-triphosphate triethylammonium salt), produced photoreceptor apoptosis in mice. They also noted that BzATP-mediated cell death was not present in P2X7r knockout mice. There is some evidence that P2X receptors are involved with cell loss in retinal degeneration. In the *rd1* mouse, Puthussery and Fletcher (2009) found that intravitreal injection of the P2X antagonist, PPADS (pyridoxalphosphate-6-azeophenyl-2'-4'-disulfonic acid tetrasodium salt), during post-natal days 14-21 was neuroprotective and reduced photoreceptor cell death. Zhang *et al*.

(2005) discovered that BzATP application caused an increase in the intracellular calcium concentration ($[Ca^{2+}]_i$) in RGCs *in vitro* and prolonged application caused death. They also showed that when BzATP was applied with the P2X antagonist brilliant blue (BBG), the rise in $[Ca^{2+}]_i$ was prevented. Similar results were obtained in rat retina; RGC death was triggered when retinas were treated *in vivo* with BzATP and this effect was blocked by BBG (Hu *et al*. 2010).

1.4.2: RGCs in rd1 Mice form P2X7r Pores

Tochitsky *et al*. (2014) were able to restore light-driven activity in a subset of RGCs (photosensitization) and improve vision-guided behaviours in blind *rd1* mice by intraocular injection of a light-sensitive azobenzene "photoswitch" molecule called DENAQ (403 Da). Subsequently, the same group (Tochitksy *et al*. 2016) demonstrated that the restored responses were due to loading of DENAQ into RGCs via P2X7r pores and was predominantly associated with OFF RGCs. TNP-ATP (2'-3'-*O*-(2,4,6-Trinitrophenyl)adenosine-5'-triphosphate tetra(triethylammonium) salt) and PPADS (non-selective P2Xr antagonists) and A740003 (a selective P2X7r antagonist) reduced or blocked DENAQ loading. Polymerase chain reaction (PCR) analysis showed the gene encoding P2X7r was upregulated in *rd1* compared to wt mice retina. DENAQ loading of RGCs in *rd1* retinas did not require ATP or P2X agonist application, and treatment with apyrase (an enzyme that degrades extracellular ATP) reduced photosensitization. This suggested that there is elevated extracellular ATP in *rd1* retinas that is sufficient to induce P2X7r pore formation in RGCs. In wt mice, DENAQ did not load RGCs and BzATP (a P2X7r selective agonist) application did not produce loading. This suggests

that there is some feature unique to *rd1* retinas that leads to up-regulation of P2X7r and pore formation, a feature that is not produced by activation of P2X7r in wt retinas. Tochitsky *et al*. (2016) performed additional experiments to assess the loading of RGCs in *rd1* and wt retinas using another molecule of comparable size and charge: YO-PRO-1. This is a cationic membrane-impermeant dye that becomes fluorescent when it interacts with nucleic acid (North 2002) and is known to enter cells through P2X7r pores (Virginio *et al.* 1999). Tochitsky *et al.* (2016) found YO-PRO-1 loaded OFF RGCs in *rd1* but not wt retinas, and the loading in *rd1* retinas was reduced by P2X7r antagonists and apyrase.

1.5: Intracellular Calcium and Calcium Imaging

Calcium ions (Ca^{2+}) are important intracellular secondary messengers and free (unbound) intracellular Ca^{2+} concentration ($[Ca^{2+}]_i$) is maintained at a low level (< 200 nM) which is ~10,000-fold less than the $[Ca^{2+}]$ in the extracellular space (Carafoli *et al*. 2001). Mechanisms to maintain low $[Ca^{2+}]_i$ include efflux through Ca^{2+} ATPase pumps or storage in internal compartments such as the endoplasmic reticulum and mitochondria (Berridge *et al*. 2000). Extreme or prolonged elevation of $[Ca^{2+}]_i$ has been shown to lead to cell death (Orrenius and Nicotera 1994), and during retinal degeneration, elevated $[Ca^{2+}]_i$ has been implicated in photoreceptor cell death (Kulkarni *et al*. 2016). As described above, increased $[Ca^{2+}]_i$ has been associated with RGC death produced by P2X7r activation (Zhang *et al.* 2005, Hu *et al*. 2010).

Free $[Ca^{2+}]_i$ can be monitored using calcium indicator dyes. The most commonly used dye, fura-2, shows changes in emission (at 510 nm) at different excitation wavelengths of light, increasing in fluorescence with increased $[Ca^{2+}]_i$ during 340 nm

excitation and decreasing in fluorescence with increased $[Ca^{2+}]_i$ during 380 nm excitation (Grynkiewicz *et al.* 1985). Taking the ratio of the emission fluorescence at each excitation wavelength provides for a qualitative or even quantitative estimate of $[Ca^{2+}]_i$ (Tsien 1989). An advantage of such ratiometric imaging is that it corrects for differences in dye loading in cells or over time.

A limitation of calcium imaging using dyes is the challenges faced by loading dye into cells. A commonly used form, acetomethoxy (AM) ester dyes (e.g. fura-2 AM) renders dyes membrane permeable (Tsien 1981). Although AM dye loading works well *in vitro*, it typically does not work well in intact tissue preparations (Baldridge 1996). One solution is to use electroporation (Bonnot *et al*. 2005, Yu *et al.* 2009), where an applied strong but brief electrical field opens transient pores in cell plasma membranes (originally designed to facilitate the transfer of genetic material into cells; Neumann *et al*. 1982) allowing the influx of dye (such as the water soluble but membrane impermeable form of fura-2, fura-2 pentapotassium salt).

1.6: Hypothesis and Objectives

Inherited retinal degenerations are retinopathies involving a loss or dysfunction of genes associated with photoreceptor (rod or cone) viability or function, including phototransduction (Duncan *et al*. 2018). The research by Tochitsky *et al.* (2016) suggested that in the *rd1* mouse model of retinal degeneration there is prolonged activation of OFF RGC P2X7r leading to the formation of pores that are permeable to large molecules. While this provided them with a conduit for loading OFF RGCs with the photoswitch DENAQ and restoration of visual function in *rd1* mice, it might also provide

a route for Ca^{2+} influx that could lead to elevated $[Ca^{2+}]_i$ resulting in RGC dysfunction or even death. Therefore, a key objective of my thesis is to determine if the intracellular Ca^{2+} dynamics of RGCs in *rd1* mice differ from those in wt mice. I hypothesized that the presence of P2X7r pores on RGCs would lead to elevated resting $[Ca^{2+}]_i$ and enhanced elevations of $[Ca^{2+}]_i$ in the presence of kainic acid (KA, ionotropic glutamate receptor agonist). Therefore, I assessed the following research questions: Is the baseline $[Ca^{2+}]_i$ elevated in fura-2 loaded GCLn in *rd1* retinas compared to wt? Is the baseline $[Ca^{2+}]_i$ affected by purinergic drugs? Are KA-induced increases of GCLn $[Ca^{2+}]_i$ altered in fura-2 loaded GCLn in *rd1* retina compared to wt retina? Are KA-induced $[Ca^{2+}]_i$ elevations affected by purinergic drugs?

Given that Tochitsky *et al.* (2016) suggested that the P2X7r pore of RGCs in *rd1* retina was large enough to load DENAQ and YO-PRO-1, and that Rassendren *et al.* (1997) reported that P2X7r pores are sufficient to permit passage of fura-2, I was curious if this might also provide a route for fura-2 loading of RGCs. I hypothesized that fura-2 will load GCLn in *rd1* retinas through P2Xr without the need for electroporation. Therefore, I compared *rd1* and wt retinas and assessed the following research questions: Does fura-2 load GCLn of the *rd1* retina and does the loading require electroporation? Are P2Xr pores the conduit for fura-2 loading in *rd1 GCLn* and is loading blocked by P2Xr antagonism? Does YO-PRO-1 label the same population of GCLn in *rd1* retinas as fura-2 labelling?

Chapter 2: Materials and Methods

2.1: Animals

Protocols were approved by the Dalhousie University Committee on Laboratory Animals, and all procedures were performed in accordance with the regulations established by the Canadian Council on Animal Care. Mice were purchased from Charles River Laboratories (St. Constant, QC, Canada) and housed in the Carleton Animal Care Facility at Dalhousie University. C3H/HeNCrl mice (homozygous for the *Pde6b*^{rd1} mutation; henceforth referred to as *rd1*) of at least 70 days old (Stock # 025, Charles River Laboratories) were the experimental group, and wild-type C57Bl/6 mice (Stock # 027, Charles River Laboratories) were the control group. Mice were housed with up to 4 animals per cage in a 12-hr light/dark cycle and had unlimited access to food and water.

2.2: Electroretinogram in rd1 Mice

Full-field electroretinograms (ERG) were performed on a randomly selected representative subgroup of 3 *rd1* mice to assess the retinal response to light stimulus in both scotopic and photopic conditions. The *rd1* mice were dark adapted for >12 hours, and scotopic recording were completed first followed by photopic recording in room lighting. Mice were anesthetized with an intraperitoneal injection of Ketamine/Xylazine (4.3 ml sterile 0.9% saline, 0.45 ml Ketamine, 0.25 ml Xylazine; CDMV. Inc. St-Hyacinthe, QC, Canada) at 10 µL/g in dim red light. The pupils were dilated with topical application of cyclopentolate HCl 1% (Alcon, Fort-Worth, Tx, USA). The mouse was placed on the ERG stage and body temperature maintained between 32-34^{o}C using a heating pad and monitored rectally. A platinum subdermal electrode (Neruoline

Subdermal; Ambu; Ballerup, Denmark) was placed into the skin between the eyes (reference) and one into the hind leg (ground). To maintain hydration and conductivity, Tear Gel (Novartis, Alcon) was applied to the eyes, and one active ERG electrode (Dawson-Trick-Litzkow-plus micro-conductive fiber; Diagnosys, Littleton, MA, USA) was placed on the cornea of each eye. Corneal electrode signals were amplified 5000-fold using a differential amplifier (0.3-300 Hz bandwidth; P511 AC Amplifier, Grass Instruments). An A/D instrument (PCI 6281 board, National Instruments, Austin, TX, USA) was used to digitize 500 sample points at a rate of 1000 Hz. Recording were collected using custom-written acquisition software (LabView 8.5; National Instruments; Austin, TX, USA). Flash stimuli were generated by a Ganzfeld stimulator (LKC Technologies, Gaithersburg, MD, USA) which produced a maximum integrated luminance of 10 log cd s m^2. Under scotopic conditions, neutral density filters (Kodak Wratten, Rochester, NY, USA) were used to attenuate the stimulus strength by 1.0 or 2.0 log units. A series of 10 flashes were acquired at 6 s interval for each luminance setting (log 2.0, 1.0, or no attenuation). Subsequently, mice underwent five minutes of light adaptation where the Ganzfeld background was illuminated fully (intensity of 1.5 log cd m^2) with room lights turned on. The 10-flash series was acquired at 1.5 s interval. Total acquisition time was approximately 4 minutes. Mice were sacrificed following ERG acquisition using a lethal intraperitoneal injection of sodium pentobarbital (Euthanyl; CDMV. Inc., St-Hyacinthe, QC, Canada) at 2.4 mg/kg.

2.3: Tissue Preparation and Fura-2 Loading

Mice were sacrificed at the time of each experiment with a lethal intraperitoneal injection of sodium pentobarbital (2.4 mg/kg Euthanyl, CDMV). Eyes were quickly enucleated and placed in room temperature Hank's Balanced Salt Solution (HBS, 10 mM HEPES, pH 7.2; Sigma-Aldrich, St. Louis, MO, USA) bubbled with 100% oxygen (Praxair, Dartmouth, NS, Canada).

2.3.1: Ex vivo Intravitreal Injection and Electroporation

The calcium-sensitive dye, fura-2, was injected into the vitreous of *rd1* or wt enucleated eyes. A hole was made through the optic disc with a 25 G needle and the fura-2 (750 nL of 20 mM fura-2 pentapotassium salt solution; Invitrogen Thermo Fisher Scientific, Eugene, OR, USA or Santa Cruz Biotechnology, Inc, Dallas, TX, USA) was injected into the vitreous chamber with a Hamilton microliter syringe. In a subset of *rd1* and wt eyes, electroporation was subsequently performed. For electroporation, Tweezertrodes^{TM} (BTX Harvard Apparatus, Holliston, MA, USA) were positioned on the globe with the cathode on the cornea and anode on the posterior pole. Five square wave 10 ms pulses at 30 V were applied with the ECM 830 electroporation system (BTX Harvard Apparatus). Eyes were placed in oxygenated HBSS for at least 20 minutes following injection or injection + electroporation prior to retinal isolation.

Retinal isolation from enucleated eyes was performed in oxygenated HBSS. A full thickness puncture was made posterior to the limbus of the enucleated eye with a #11 scalpel blade. An incision was made around the circumference of the eye using surgical scissors to separate the posterior globe from the anterior segment and lens. The retina was

isolated from the choroid and sclera, and the vitreous carefully removed using forceps. The retinas were mounted GCL-side up on black filter paper (Millipore Sigma, Etobicoke, ON, Canada) and maintained in oxygenated HBSS for at least 60 min prior to being transferred to a microscope-mounted superfusion chamber for calcium imaging. Following imaging, some retinas that were loaded with fura-2 by intravitreal injection were incubated in the P2X7r pore-permeant dye YO-PRO-1 (100nM; Molecular probes, Eugene, OR, USA) for 15 min followed by a 10 min wash in oxygenated HBSS and imaged further.

2.3.2: Isolated Retina Incubation

Some retinas were loaded with fura-2 by incubation. The retinas of enucleated eyes of *rd1* or wt mice were isolated (as described above) and then incubated in fura-2 (20 μL of 5 mM fura-2 salt solution) for 15 min. The retinas were then moved to the imaging chamber and allowed to wash in oxygenated HBSS for 10 min prior to imaging.

2.3.3: Effect of P2 Receptor Antagonists on Fura-2 Loading

The possible involvement of P2X7 receptor pores for fura-2 loading was assessed by intravitreal injection (750 nL) of antagonist into enucleated eyes prior to injection with fura-2 salt solution, or by concurrent incubation of isolated retinas in antagonist and fura-2 salt solution for 15 min followed by a 10 min wash with oxygenated HBSS. The drugs used are described in Table 2.1.

Table 2.1. P2 receptor antagonists for fura-2 loading experiments.

Drug	Type	Application	Concentration	Estimated Intravitreal Concentration	Solubilized	Supplier
A740003	P2X7 selective	Intravitreal injection	66.7 µM	10 µM	DMSO and HBSS	Cayman
PPADS	Non-selective P2	Intravitreal injection	6.7 mM	1 mM	HBSS	Cayman
TNP-ATP	Non-selective P2X	Intravitreal injection	3.3 mM	500 µM	HBSS	Tocris
		Incubation	500 µM	n/a	HBSS	

Legend: A740003, N-(1-[[(Cyanoamino)(5-quinolinylamino)methylene]amino]-2,2-dimethylpropyl)-3,4-dimethoxybenzeneacetamide; PPADS, Pyridoxalphosphate-6-azeophenyl-2'-4'-disulfonic acid tetrasodium salt; TNP-ATP, 2'-3'-O-(2,4,6-Trinitrophenyl)adenosine-5'-triphosphate tetra(triethylammonium) salt.

Cayman, Cayman Chemical Company, Denver, CO, USA; Tocris, Tocris Bioscience, Bristol, United Kingdom.

2.4: Calcium Imaging

Isolated retinas were placed in a microscope-mounted chamber and superfused with oxygenated HBSS at a rate of ~1.5 ml/min. Neurons in the GCL (GCLn) of isolated retinas were visualized using a 40X water-immersion objective (0.80 numerical aperture, Achroplan; Carl Zeiss Meditec, Oberkochen, Germany) and images were captured using a cooled CCD camera (Sensicam PCO, Kelheim, Germany). Fura-2 fluorescence was produced using the light from a 75-W xenon lamp (Sutter Instruments, Novato, CA, USA) and band-pass filtered (XF04 set, excitation 340 or 380 nm; emission 510 nm; dichroic >430 nm; Omega Optical, Brattleboro, VT, USA) and used for ratiometric fura-2 calcium imaging. Image pairs at 340 and 380 nm excitation (both with 510 nm emission) were collected using Axon Imaging Workbench 4.0 software (Molecular Devices; Sunnyvale, CA, USA). This software generated ratiometric images from the recording of fura-2 fluorescence at the two excitation wavelengths. Image acquisition occurred at

frequency of one frame per 20 s which was increased to a frequency of one frame per 5 s during periods when the fura-2 ratio values increased due to transient increases of $[Ca^{2+}]_i$. YO-PRO-1 fluorescence was produced using a different band-pass filter (XF100 set, excitation 475 nm; emission 535 nm; dichroic >430 nm; Omega Optical, Brattleboro, VT, USA).

For each experiment, the resting fura-2 ratios were recorded for 5 min (oxygenated HBSS superfusion). The imaged GCLn were excited by the ionotropic (AMPA/kainate) agonist kainic acid (KA; 50 μM in HBSS; Hello Bio, Princeton, NJ, USA or Research Biochemicals International, Natick, MA, USA) via superfusion for 30 s. Retinas were washed with HBSS for at least 15 min following any treatment.

2.4.1: Effect of P2 Receptor Drugs on Baseline and KA-induced Calcium Transients

The effect of various P2 drugs and enzymes (see Table 2.2) on baseline or KA-induced calcium transients were tested. In each case, drug(s) were applied to the retina via superfusion.

Table 2.2. P2 receptor modulating drugs and enzymes for baseline and KA-induced calcium transient experiments.

Drug	Type	Concentration	Solubilized	Supplier
A740003	P2X7 antagonist	10 μM	DMSO and HBSS	Cayman
Apyrase	Hydrolyzes ATP	5 units/ml	HBSS	Sigma-Aldrich
BzATP	P2X7 agonist	250 μM	HBSS	Sigma-Aldrich
ATPγS	Non-hydrolyzable ATP analogue, P2 agonist	185 μM	HBSS	Tocris

Legend: A740003, *N*-(1-[[(Cyanoamino)(5-quinolinylamino)methylene]amino]-2,2-dimethylpropyl)-3,4-dimethoxybenzeneacetamide; BzATP, 2'(3')-*O*-(4-Benzoylbenzoyl)adenosine 5'-triphosphate triethylammonium salt; ATPγS, Adenosine-5'-(γ-thio)-triotriphosphate tetralithium salt.

Cayman, Cayman Chemical Company, Denver, CO, USA; Sigma-Aldrich, Sigma Aldrich Canada, Oakville, ON, CAN; Tocris, Tocris Bioscience, Bristol, United Kingdom.

2.5: Data Analysis

2.5.1: Electroretinogram

ERG waveforms were analyzed using a custom-design Matlab toolbox (Mathworks, Natick, MA, USA) written by Dr. Francois Tremblay and Matt Boardman. Series recordings for right and left eyes were averaged within each mouse and the recording series for each stimulus intensity were graphed using Microsoft Excel (Redmond, WA, USA). Dr. Margaret Luke provided the wildtype ERG recordings and measured the amplitude and implicit time of the a- and b- wave (descriptive data not shown). This would have been done in the *rd1* recordings; however, there was essentially no ERG response and deviations from baseline were regarded as noise.

2.5.2: Fura-2 Loading and Ca^{2+} Imaging

For GCLn loading experiments, retinal images were acquired using Axon Imaging Workbench 4.0 (Molecular Devices). Using the 380 nm excitation wavelength image, the total cells/field of view (cells/FOV) were counted for each retina. Each retina was n = 1. The mean cells/FOV was calculated for each experimental group. In the YO-PRO-1 loading experiments, the corresponding FOV for the fura-2 image of the same retina was overlaid with the YO-PRO-1 image to assess alignment of the loaded cells.

Axon Imaging Workbench 4.0 (Molecular Devices) was used for both recording and analysis of the calcium imaging experiments. After the experiments were completed, KA-responding fura-2 labelled GCLn within the FOV were selected in the recordings as regions of interest (ROIs) and the fluorescence ratio was recorded over time. The resting fura-2 ratio (also referred to as baseline $[Ca^{2+}]_i$) for each ROI was generated from the averaged values of the first 15 images obtained before drug application. The mean baseline $[Ca^{2+}]_i$ was calculated for each retina and compared between experimental groups. The peak calcium transient for each ROI per drug application was determined and the mean peak calcium transient was calculated per retina and compared between experimental groups. Each retina was n = 1.

Graphing and statistical analysis were performed using Prism 8 software (GraphPad; La Jolla, CA, USA). The data were analyzed by repeated-measured ANOVA followed by Tukey's multiple comparisons test, one-way ANOVA followed by Tukey's multiple comparisons test, paired t-test, or unpaired t-test when applicable. Data are displayed as mean ± standard deviation (SD) and the alpha value used was 0.05.

Chapter 3: Results

The *rd1* mouse model of inherited retinal degeneration has proven useful for research that seeks to restore light sensitivity to neurons in the presumably blind *rd1* eye. In fact, the presence of P2Xr pores has been exploited to load retinal ganglion cells (RGCs) with light-sensitive molecules (Tochitsky *et al.* 2016), thereby restoring retinal light sensitivity. However, the presence of P2Xr pores could alter normal intracellular Ca^{2+} dynamics with uncertain consequences. The objective of this work was to determine if the P2Xr pores expressed by ganglion cell layer neurons (GCLn) in the *rd1* mouse retina provide a conduit for calcium indicator dye loading and/or alter intracellular Ca^{2+} dynamics.

3.1: ERGs in rd1 Mouse

The *rd1* mouse is an animal model of inherited retinal degeneration and is characterized by progressive photoreceptor cell death that leads to retinal disfunction and blindness by wean age (~ post-natal day 20) (Bowes 1990, Stasheff 2008). The animals used in the study were at least 3 months old to ensure that retinal degeneration was fully developed. To confirm the *rd1* mice were blind at this age, full-field electroretinogram tests (ERG) were performed on 3 *rd1* mice. Full-field ERGs record the light-induced mass electrical response of the retina produced under scotopic (dark) and photopic (bright) conditions with different background and light stimulus intensities. As illustrated in Figure 3.1, there was essentially no ERG response for each *rd1* animal under both scotopic and photopic conditions with various stimuli intensities compared to wt responses in similar conditions. For the *rd1* recordings, the small deviations from

baseline were regarded as noise. These data confirmed that the retinas of these *rd1* mice had degenerated.

3.2: Fura-2 Loading in rd1 and wt Retinas

It has been suggested that some RGCs in *rd1* retina express P2X receptors that form pores allowing large molecules to enter (Tochitsky *et al.* 2016). We tested the hypothesis that the calcium-indicator dye fura-2, normally membrane-impermeable, could load GCLn in *rd1* retina via P2Xr pores. To evaluate this, two different dye application techniques were used: intravitreal injection and retina incubation.

As illustrated in Figure 3.2A, there was limited loading of the GCLn following intravitreal injection of fura-2 salt in wt mice. Intravitreal injection of fura-2 into *rd1* mice resulted in much greater labelling (Figure 3.2B). Fura-2 can be loaded into GCLn by intravitreal injection followed by electroporation (Daniels and Baldridge 2010). The extent of fura-2 loading in wt and *rd1* retinas subject to electroporation was similar (Figure 3.2C,D) and was comparable to the loading achieved without electroporation in *rd1* (Figure 3.2B).

Similar results were found in all retinas studied (Figure 3.2E, mean ± SD summarized in Table 3.1). On average, 124 ± 35 (mean ± SD) cells/field of view (FOV) were loaded in *rd1* retinas compared to 24 ± 14 cells/FOV in retinas of wt mice. When electroporation was used, 84 ± 36 cells/FOV were loaded in *rd1* retinas and 104 ± 39 cells/FOV in the case of wt. The mean number of cells/FOV loaded with fura-2 was

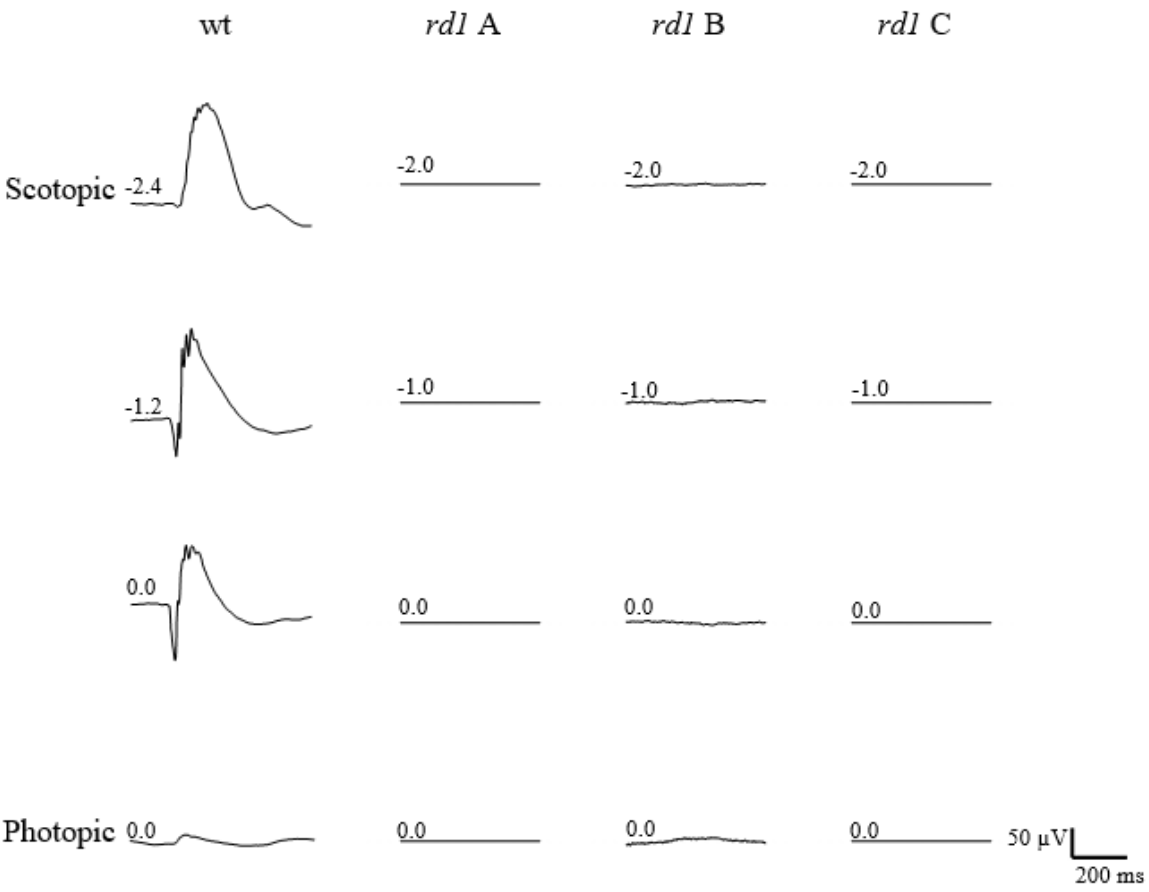

Figure 3.1: ERGs of *rd1* mice were absent compared to wt. Example waveforms of ERG recordings comparing ERGs in wt mice and three *rd1* mice. There was no background light in the Ganzfeld dome for scotopic recordings, and maximum background light in the Ganzfeld dome for photopic recordings. Flash stimulus intensities for *rd1* experiments were 2.0, 1.0, and 0.0 log attenuation and for wt were 2.4, 1.2, and 0.0 log attenuation of the maximum flash luminance 10 log cd s m^2.

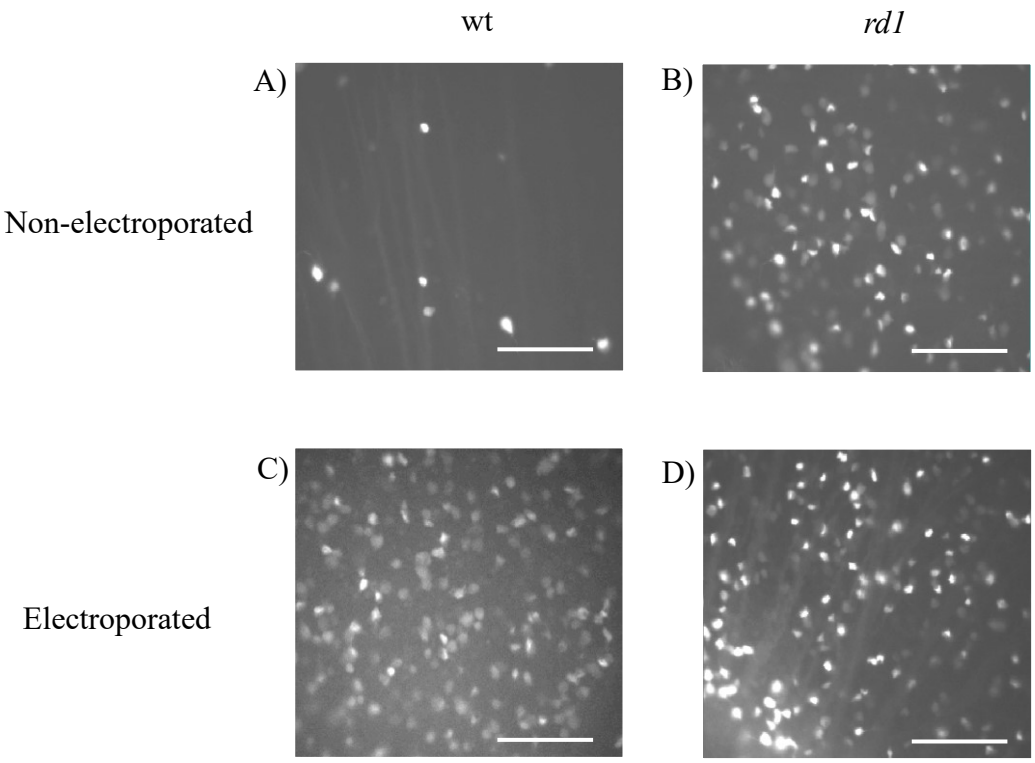
wt
rd1
A)
B)
Non-electroporated
C)
D)
Electroporated

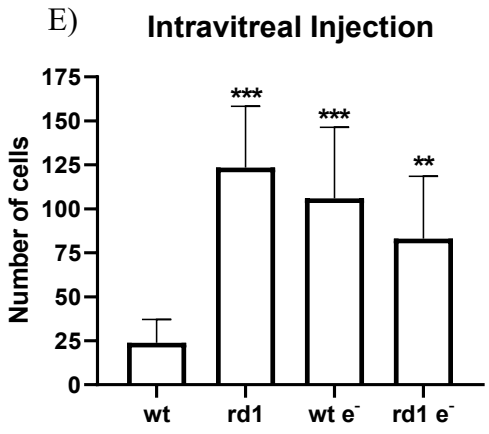
E)
Intravitreal Injection
Number of cells
175
150
125
100
75
50
25
0
***
***
**
wt
rd1
wt e-
rd1 e-

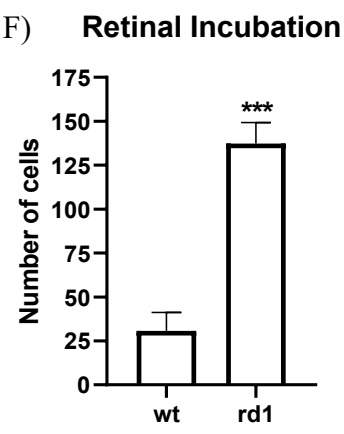
F)
Retinal Incubation
Number of cells
175
150
125
100
75
50
25
0
***
wt
rd1

Figure 3.2: Fura-2 loading of the GCL is greater in *rd1* retina. (A-D) Representative fluorescence images (380 nm excitation; 510 nm emission) of fura-2 loading in the GCL following intravitreal injection of eyes from (A) wt and (B) *rd1* mice or following intravitreal injection and electroporation of (C) wt and (D) *rd1* mice. Scale bars = 50 µm. (E) Mean (± SD) fura-2 loading following intravitreal injection (wt, n = 6; *rd1*, n = 40) and following intravitreal injection and electroporation (wt e^-, n = 24; *rd1* e^-, n = 21). ** $p<0.01$, *** $p<0.001$ compared to wt (one-way ANOVA, Tukey's multiple comparison test). (F) Mean (± SD) loading following incubation of isolated retina in fura-2 (wt n = 4; *rd1*, n = 3). *** $p<0.001$ (unpaired t-test).

greater ($p<0.01$; one-way ANOVA with Tukey's multiple comparison test) in *rd1* (not electroporated) and electroporated (both *rd1* and wt) retinas compared to wt (not electroporated) retinas. There was no significant difference ($p>0.05$; one-way ANOVA with Tukey's multiple comparison test) between fura-2 loading of *rd1* (not electroporated) and electroporated (both *rd1* and wt) retinas.

To further assess fura-2 loading of the GCL in *rd1* retina, retinas were first isolated and then incubated in fura-2 solution (Figure 3.2F, mean ± SD summarized in Table 3.1). This approach produced similar results to those observed using intravitreal injection. There was significantly more fura-2 loading of the GCL in *rd1* than in wt retinas ($p<0.05$; unpaired t-test). Mean cell loading for each group was: *rd1* 138 ± 12 cells/FOV, wt 31 ± 11 cells/FOV.

Table 3.1. Fura-2 loaded GCLn cell counts for *rd1* and wt intravitreal injection (± electroporation) and retinal incubation fura-2 loading techniques. Data represented are mean ± SD cells/FOV (cells per field of view), one-way ANOVA with Tukey's multiple comparison test or unpaired t-test. ** $p<0.01$, *** $p<0.001$ compared to wt, n = number of retinas.

Group	Fura-2 loaded GCLn (mean ± SD cells/FOV)			
	Intravitreal Injection		Retinal Incubation	
wt	24 ± 14	(n = 6)	31 ± 11	(n = 4)
rd1	124 ± 35***	(n = 40)	138 ± 12***	(n = 3)
wt e^-	104 ± 39***	(n = 24)	-	-
rd1 e^-	84 ± 36**	(n = 21)	-	-

To determine if the increased fura-2 loading in *rd1* retina was mediated by the P2Xr pores, the effect of antagonist acting on P2X receptors was tested. In experiments using the intravitreal injection of fura-2, A740003 (a P2X7r antagonist, 66.7 μM), PPADS (a P2r antagonist, 6.7 μM), or TNP-ATP (a P2Xr antagonist, 3.3 mM) was injected intravitreally prior to fura-2 (Figure 3.3A, mean ± SD summarized in Table 3.2). None of the antagonists caused a reduction in fura-2 loading in *rd1* retina; in fact, there was significantly more fura-2 loading in the presence of A740003 compared to *rd1* controls ($p<0.001$; one-way ANOVA, Tukey's multiple comparison test). Mean fura-2 loading was: A740003 222 ± 32 cells/FOV, PPADS 155 ± 35 cells/FOV, TNP-ATP 176 ± 31 cells/FOV. Similar results were obtained when isolated retinas were incubated in the presence of TNP-ATP (500 μM incubation) (Figure 3.3B). TNP-ATP did not reduce fura-2 loading in *rd1* retinas ($p>0.05$; unpaired t-test). Mean fura-2 loading in the presence of TNP-ATP was 112 ± 61 cells/FOV.

Table 3.2. Fura-2 loaded GCLn cell counts for *rd1* in the presence of antagonists (A740003, PPADS, TNP-ATP) for intravitreal injection and retinal incubation fura-2 loading techniques. Data represented are mean ± SD cells/FOV, one-way ANOVA with Tukey's multiple comparison test or unpaired t-test. *** $p<0.001$ more loading compared to *rd1,* n = number of retinas

Group	Fura-2 loaded GCLn (mean ± SD cells/FOV)			
	Intravitreal Injection		Retinal Incubation	
rd1 control	124 ± 35	(n = 40)	138 ± 12	(n = 3)
A740003	222 ± 32***	(n = 4)	-	-
PPADS	155 ± 35	(n = 5)	-	-
TNP-ATP	176 ± 31	(n = 3)	112 ± 61	(n = 3)

P2Xr pores are permeable to the nuclear dye YO-PRO-1 (Virginio *et al.* 1999, Khakh *et al*. 1999) and Tochitsky *et al.* (2016) found enhanced loading of YO-PRO-1 in certain GCLn in the *rd1* retina. I assessed and compared YO-PRO-1 (100 nM) loading in *rd1* GCLn loaded first with fura-2 through intravitreal injection (Figure 3.4A-C). As illustrated in Figure 3.4B, YO-PRO-1 labelled the nuclei of both presumptive neurons and vascular cells (arrows) in the GCL of *rd1* retinas. However, YO-PRO-1 never colocalized with fura-2 (Figure 3.4C) (identical results were found in 4 other *rd1* retinas).

Collectively, these results suggest that even though fura-2 can enter GCLn more readily in *rd1* retina compared to wt, and it is unlikely that P2Xr pores are the conduit for fura-2.

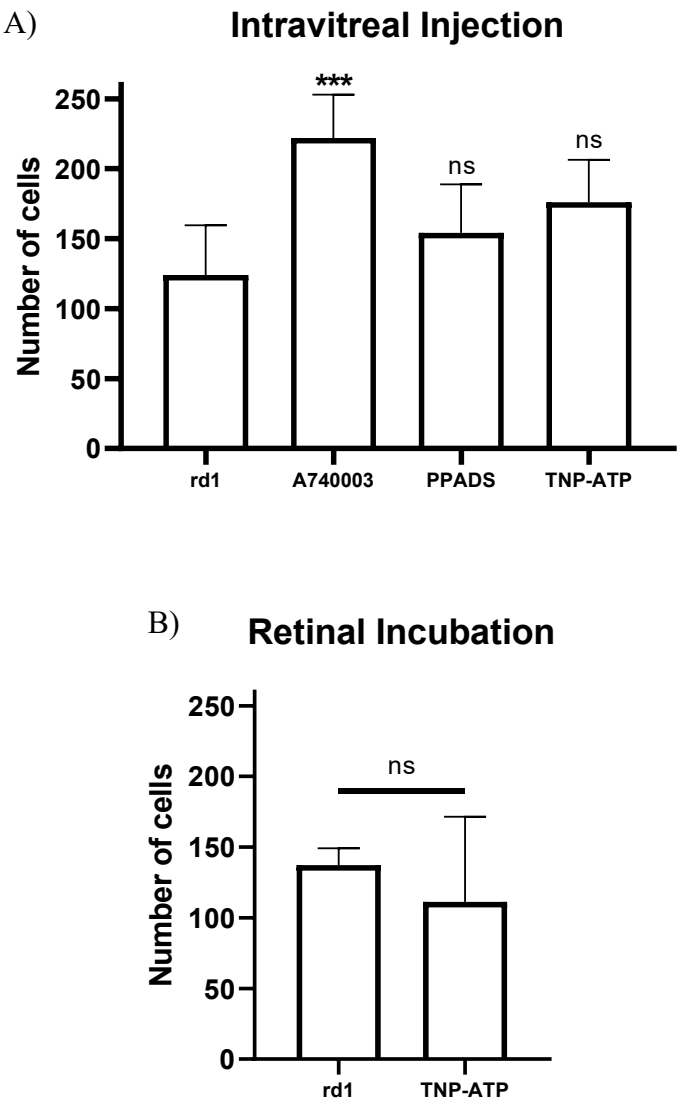

Figure 3.3: Fura-2 loading of GCL in *rd1* retina is not blocked by antagonists of P2X receptors. (A) Mean (± SD) fura-2 loading (by intravitreal injection) in *rd1* retinas (n = 40) and in *rd1* retinas following a prior intravitreal injection of 66.7 μM A740003 (n = 4), 6.7 μM PPADS (n = 5) or 3.3 mM TNP-ATP (n = 3). *** $p<0.001$, ns $p>0.05$ compared to *rd1* (one-way ANOVA, Tukey's multiple comparison test). (B) Mean (± SD) loading following incubation of isolated *rd1* retina in fura-2 alone (n = 3) or in the presence of fura-2 and 500 μM TNP-ATP (n = 3). ns $p>0.05$ (unpaired t-test).

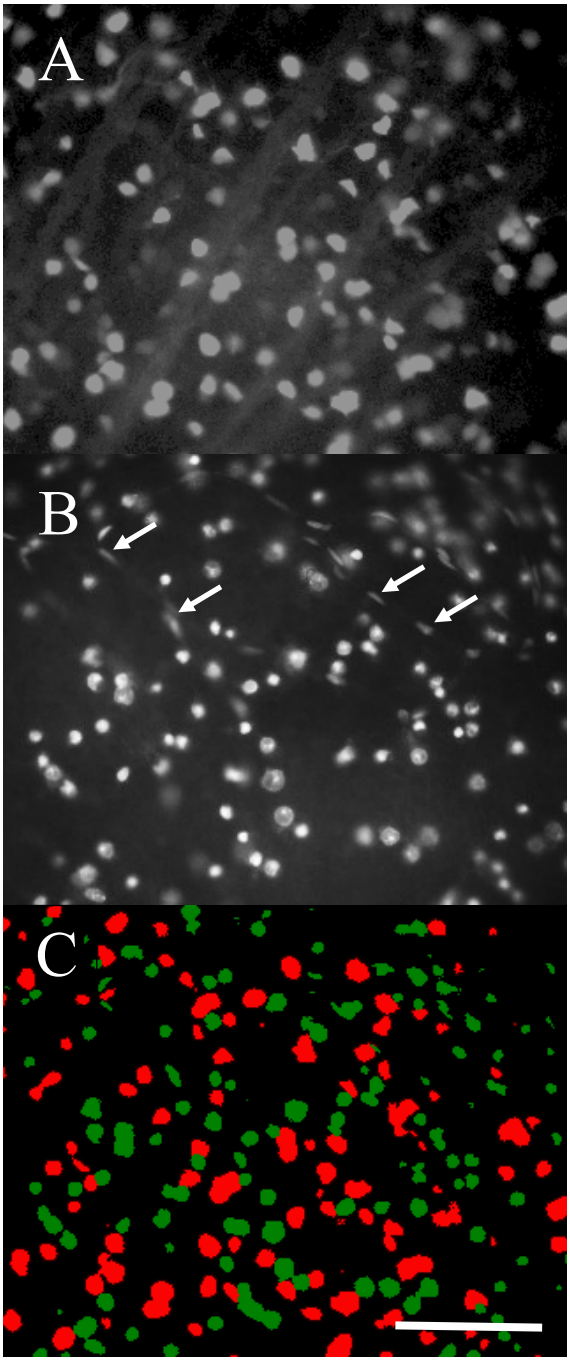

Figure 3.4: Fura-2 and YO-PRO-1 loading does not colocalize in the *rd1*.

Representative fluorescence images of (A) fura-2 loading, (B) YO-PRO-1 loading, and (C) overlay of A (fura-2, red) and B (YO-PRO-1, green) in the GCL of *rd1* retina. Arrows indicate presumptive labelling of vasculature cell nuclei by YO-PRO-1. Scale bar = 50 μm.

3.3: Calcium Dynamics

Although the loading of fura-2 in the GCL of *rd1* mice did not appear to be mediated by P2X pores, such loading suggests the presence of another conduit in GCLn of *rd1* retinas that could lead to increased $[Ca^{2+}]_i$. Therefore, I compared the resting fura-2 ratio (a measure of baseline $[Ca^{2+}]_i$) in GCLn in *rd1* and wt retina in both electroporated and non-electroporated eyes (Figure 3.5A; mean ± SD summarized in Table 3.3). There was no significant difference between the mean resting fura-2 ratio of GCLn in *rd1* and wt retinas, or between retinas from electroporated vs. non-electroporated eyes ($p>0.05$; one-way ANOVA, Tukey's multiple comparison test). These data indicate that there was no difference between baseline $[Ca^{2+}]_i$ in GCLn in *rd1* and wt retinas in both electroporated and non-electroporated eyes.

Table 3.3. Baseline fura-2 fluorescence ratio in *rd1* and wt GCLn with the intravitreal injection (± electroporation) fura-2 loading technique. Data represented are mean ± SD, one-way ANOVA with Tukey's multiple comparison test. n = number of retinas.

Group	Baseline fura-2 fluorescence ratio (mean ± SD)	
rd1	0.27 ± 0.03	(n = 34)
rd1 e^-	0.28 ± 0.04	(n = 9)
wt e^-	0.25 ± 0.04	(n = 20)
Wt	0.26 ± 0.03	(n = 6)

To test the possible impact of P2Xr on baseline $[Ca^{2+}]_i$ in fura-2-loaded GCLn in *rd1* retina, I examined the effect of purine receptor drugs on the resting fura-2 ratio in GCLn from *rd1* (not electroporated) and wt (electroporated) retinas. The compounds tested were: A740003 (a selective P2X7r antagonist, 10 μM), BzATP (a P2X7r agonist,

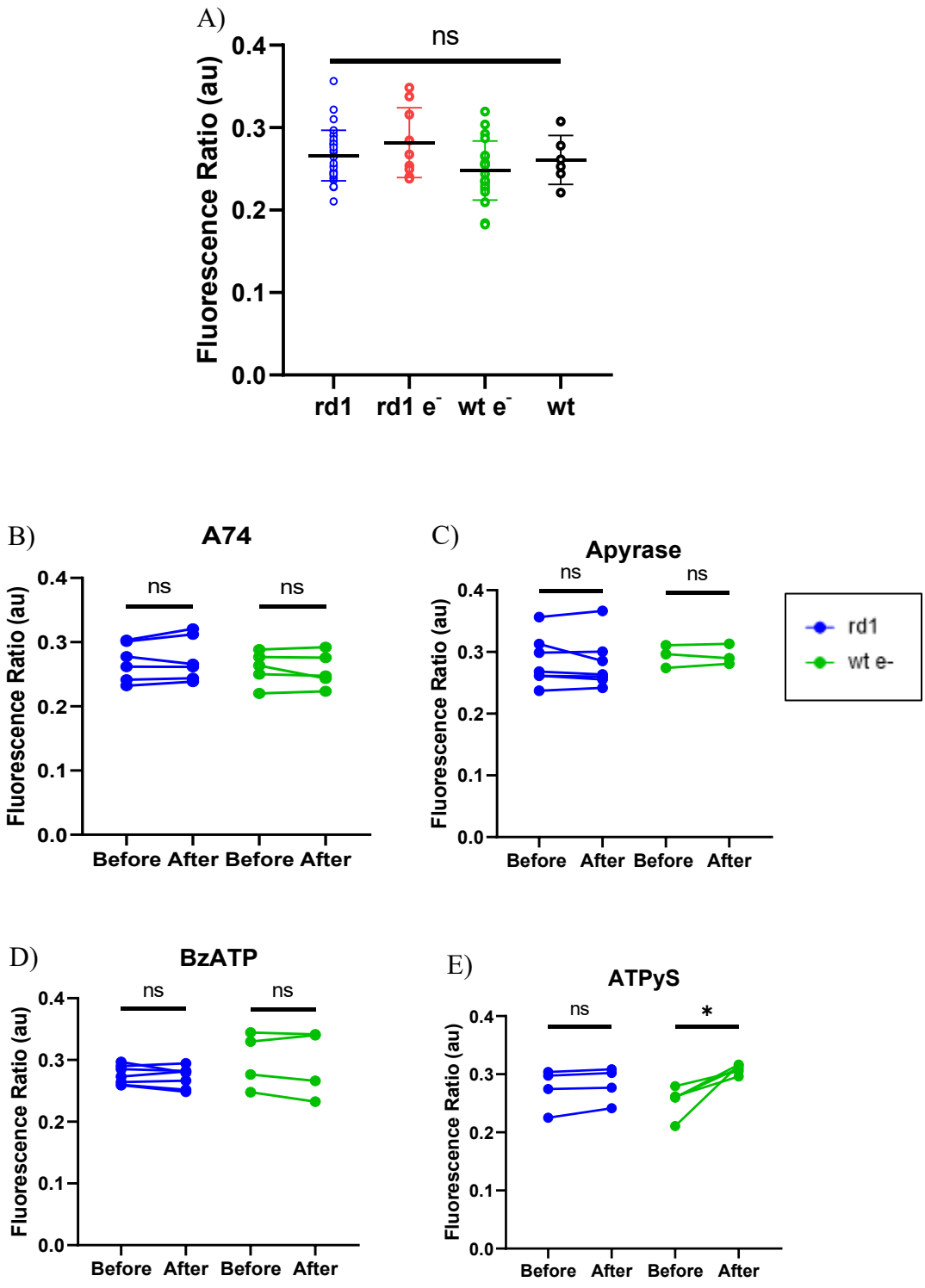
A)
ns
Fluorescence Ratio (au)
0.4
0.3
0.2
0.1
0.0
rd1
rd1 e-
wt e-
wt
B)
A74
ns
ns
Fluorescence Ratio (au)
Before After Before After
C)
Apyrase
ns
ns
rd1
wt e-
Fluorescence Ratio (au)
Before After Before After
D)
BzATP
ns
ns
Fluorescence Ratio (au)
Before After Before After
E)
ATPyS
ns
*
Fluorescence Ratio (au)
Before After Before After

Figure 3.5: Resting GCLn $[Ca^{2+}]_i$ in *rd1* retinas is not different from wt and is not affected by purine drugs. (A) Mean (± SD) resting fura-2 fluorescence ratio in GCLn from *rd1* and wt retinas, subject to intraocular injection of fura-2 or intraocular injection of fura-2 and electroporation (e^-). Each data point represents the averaged value from a single retina. ns $p>0.05$ (one-way ANOVA, Tukey's multiple comparison test). (B-E) Effect of (B) 10 μM A740003 (A74), (C) 5 units/ml apyrase, (D) 250 μM BzATP or (E) 185 μM ATPγS on resting fura-2 fluorescence ratio in GCLn from *rd1* retinas loaded with fura-2 by intraocular injection (blue) and wt retinas loaded with fura-2 by intraocular injection followed by electroporation (green). Each data point represents the averaged value from a single retina. * $p<0.05$; ns $p>0.05$ (paired t-test).

250 μM), apyrase (an extracellular ATP-degrading enzyme, 5 units/ml) and ATPγS (a P2r agonist and nonhydrolyzable form of ATP, 185 μM). Neither A740003, BzATP nor apyrase had a consistent effect on the resting fura-2 ratio in GCLn from *rd1* or wt retinas (Figure 3.5B-D) and there was no significant differences between mean data (Table 3.4; $p>0.05$; control vs. treated; paired t-test). There was a small increase in the fura-2 ratio after treatment with ATPγS in GCLn from wt (electroporated) retinas ($p<0.05$), but no effect on GCLn in *rd1* retina (Figure 3.5E, Table 3.4). These results do not support the hypothesis that GCLn from *rd1* retinas have altered sensitivity relative to wt to purinergic drugs.

Table 3.4. Baseline fura-2 fluorescence ratio in *rd1* and wt e^- GCLn before and after purinergic drug application (A740003, apyrase, BzATP, ATPγS). Data represented are mean ± SD, paired t-test. * $p<0.05$ compared to 'before'. n = number of retinas.

Drug	Baseline fura-2 fluorescence ratio (mean ± SD)					
	rd1			wt e^-		
	Control	Treated		Control	Treated	
A740003	0.27 ± 0.03	0.27 ± 0.04	(n = 6)	0.26 ± 0.03	0.26 ± 0.03	(n = 5)
Apyrase	0.29 ± 0.04	0.28 ± 0.04	(n = 7)	0.30 ± 0.02	0.30 ± 0.02	(n = 3)
BzATP	0.27 ± 0.02	0.27 ± 0.02	(n = 7)	0.30 ± 0.05	0.30 ± 0.06	(n = 4)
ATPγS	0.28 ± 0.04	0.28 ±0.03	(n = 4)	0.25 ± 0.03	0.31 ± 0.01*	(n = 5)

I next compared the Ca^{2+} dynamics of fura-2 loaded GCLn in *rd1* retinas to wt retinas during treatment with kainic acid (KA), an ionotropic glutamate receptor agonist. When applied to the retina, KA causes a transient increase of fura-2 ratio indicating a transient increase in $[Ca^{2+}]_i$. The effect of KA on GCLn from an *rd1* retina is illustrated in Figure 3.6A-C. KA (50 μM) increased the fura-2 ratio in GCLn, rising from baseline (A, before KA) to a peak (B, during KA) followed by recovery (C, after wash). Figure 3.6D illustrates fura-2 ratio values over time for 20 cells recorded in the *rd1* retina shown

in Figure 3.6A-C during KA treatment, illustrating the KA-induced rise from the baseline of fura-2 ratio, reaching a peak and then followed by a recovery back to baseline.

I first compared the peak fura-2 ratio reached by treatment with 50 μM KA in GCLn from *rd1* retinas (loaded by intraocular injection with fura-2 but not electroporated) and wt (loaded by intraocular injection followed by electroporation) (Figure 3.7A). The mean peak fura-2 ratio for GCLn from *rd1* retinas was greater compared to wt (Table 3.5; $p<0.001$; one-way ANOVA, Tukey's multiple comparison test). Similar results were obtained when *rd1* eyes were subjected to electroporation after fura-2 intraocular injection; mean peak fura-2 ratio was significantly elevated relative to wt (electroporated). These data suggest that GCLn in *rd1* retinas have enhanced elevations of $[Ca^{2+}]_i$ in response to KA relative to GCLn from wt retinas.

Table 3.5. Peak KA-induced Ca^{2+} response in *rd1* and wt GCLn (± electroporation). Data represented are mean ± SD, one-way ANOVA with Tukey's multiple comparison test. *** $p<0.001$ compared to wt e^-. n = number of retinas.

Group	KA-Induced Ca^{2+} Response (mean ± SD)	
rd1	0.50 ± 0.05***	(n = 34)
rd1 e^-	0.53 ± 0.06***	(n = 9)
wt e^-	0.40 ± 0.05	(n = 20)

To determine if the enhanced response to KA in *rd1* retinas involves P2Xr, I used the same series of purine drugs used to study baseline $[Ca^{2+}]_i$ (Figure 3.5). In most *rd1* retinas, application of A740003 (P2X7r antagonist) or apyrase (ATP-degrading enzyme) caused a decrease in the amplitude of the GCLn response (peak fura-2 ratio) produced by KA, an effect that was reversed after wash (Figure 3.7B, C). The mean GCLn response produced by KA was significantly decreased by A740003 or apyrase in *rd1* retina (Table

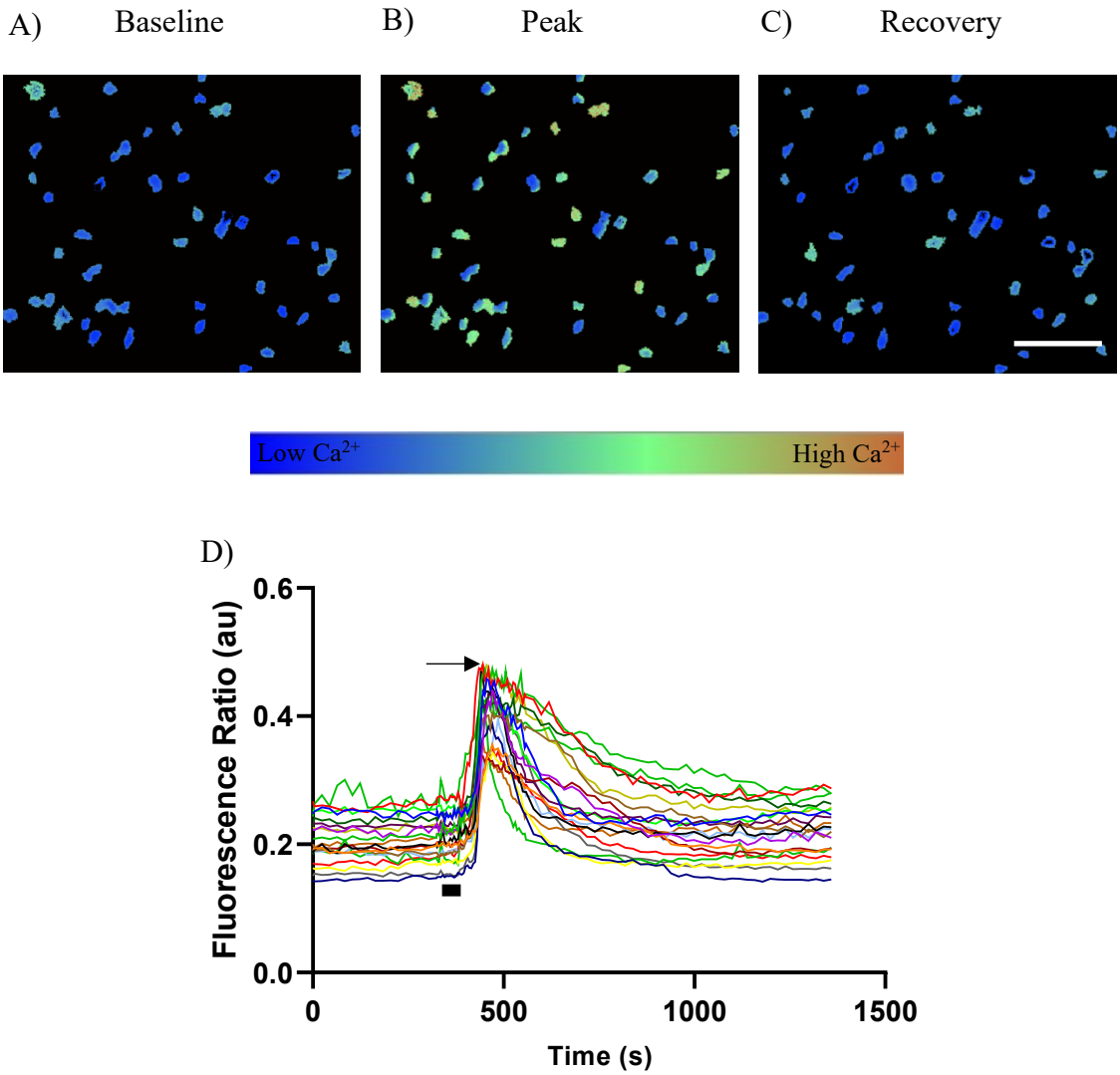

Figure 3.6: KA increases $[Ca^{2+}]_i$ in *rd1* GCLn. (A-C) Representative images illustrating Ca^{2+} responses produced by 50 µM KA in fura-2-loaded GCLn in an isolated *rd1* retina (A) before, (B) at the peak response and (C) after recovery. Scale bar = 50 µm. (D) Traces of fura-2 fluorescence ratios over time from 20 GCLn in an *rd1* retina. Bar indicates 30 sec application of KA. Black arrow indicates the peak of the KA-induced response.

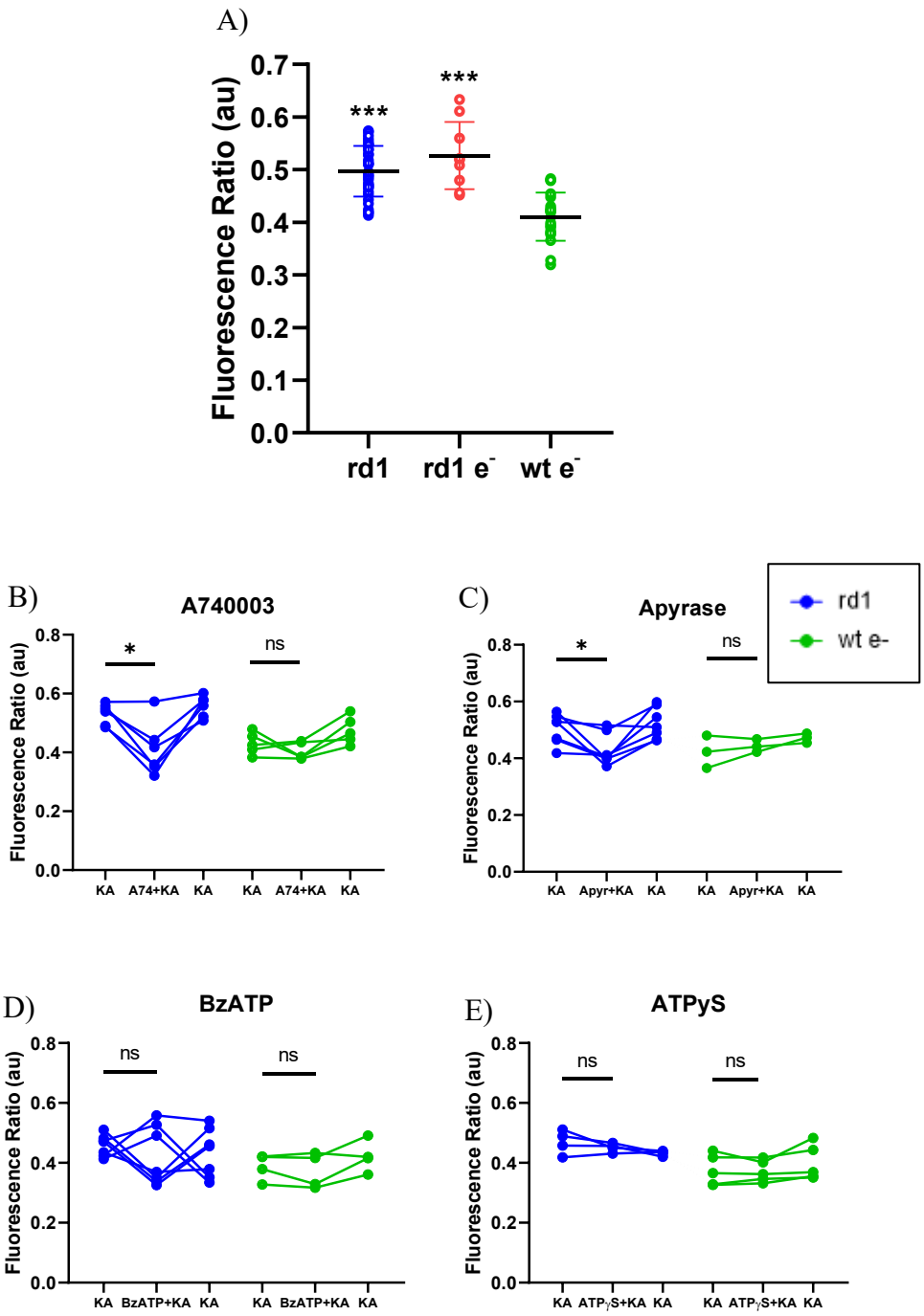
A)
Fluorescence Ratio (au)
0.7
0.6
0.5
0.4
0.3
0.2
0.1
0.0
***
***
rd1
rd1 e-
wt e-
B)
A740003
*
ns
KA A74+KA KA KA A74+KA KA
C)
Apyrase
rd1
wt e-
*
ns
KA Apyr+KA KA KA Apyr+KA KA
D)
BzATP
ns
ns
KA BzATP+KA KA KA BzATP+KA KA
E)
ATPyS
ns
ns
KA ATPγS+KA KA KA ATPγS+KA KA

Figure 3.7: KA-induced Ca^{2+} transients are enhanced in GCLn in *rd1* retina and are reduced by P2X7 antagonist or enzymatic digestion of extracellular ATP. (A) Mean (± SD) fura-2 fluorescence ratio in GCLn treated with 50 μM KA from *rd1* and wt retinas, subject to intraocular injection of fura-2 (rd1) or intraocular injection of fura-2 and then electroporated (*rd1* e^- and wt e^-). Each data point represents the averaged value from a single retina. *** $p<0.001$ compared to wt (one-way ANOVA, Tukey's multiple comparison test). (B-E) Effect of (B) 10 μM A740003 (A74), (C) 5 units/ml apyrase, (D) 250 μM BzATP or (E) 185 μM ATPγS on 50 μM KA-induced responses (increased fura-2 fluorescence ratio) in GCLn from *rd1* retinas loaded with fura-2 by intraocular injection (blue) and wt retinas loaded with fura-2 by intraocular injection followed by electroporation (green). Each data point represents the averaged value from a single retina. * $p<0.05$; ns $p>0.05$ (repeated measures ANOVA, Tukey's multiple comparison test).

3.6; $p<0.05$; one-way ANOVA, Tukey's multiple comparison test). This was not the case in wt retinas; neither A740003 nor apyrase produced a significant change in the mean GCLn response to KA (Figure 3.7B, C; $p>0.05$; one-way ANOVA, Tukey's multiple comparison test). These data suggest that antagonism of P2X7r (by A740003) or enzymatic digestion of extracellular ATP (apyrase) reduce the enhancement of GCLn responses (elevated $[Ca^{2+}]_i$) to KA in *rd1* retinas but have no effect in wt retinas. The P2X7r agonist, BzATP, and the non-hydrolyzable form of ATP, ATPγS, did not produce consistent changes in GCLn responses to KA in *rd1* or wt retinas (Figure 3.7D, E) with no difference in mean data (Table 3.6; $p>0.05$; one-way ANOVA, Tukey's multiple comparison test).

Collectively, these data (Figure 3.7) suggest that the enhanced KA-induced Ca^{2+} responses in *rd1* GCLn are due to ATP released during KA application that acts, at least in part, on P2X7 receptors. The absence of an effect of BzATP or ATPγS on KA-induced Ca^{2+} responses in GCLn in *rd1* retinas suggests that the level of ATP released during KA treatment is saturating. The lack of an effect of any of the purine drugs on KA-induced Ca^{2+} responses in GCLn in wt retinas suggests that there is an ATP-dependent cause for the enhancement of KA responses in *rd1* retinas that is not mimicked by treatment with BzATP or ATPγS of wt retinas.

If KA increases the ATP release in the *rd1* retina that enhances GCLn Ca^{2+} dynamics by acting on GCLn P2X7r, then A740003 should not only reduce the response to KA but should also block any effect of ATPγS on the KA response. However, I found that in the presence of A740003, ATPγS enhanced the KA-induced responses (Figure 3.8). These results suggest that whilst antagonism of P2X7r reduces the enhancement of

KA-induced Ca^{2+} responses, the mechanism is not simply explained by enhanced endogenous release of ATP acting on GCLn.

Table 3.6. Peak KA-induced Ca^{2+} response in *rd1* and wt e^- GCLn in the presence of purinergic drugs (A740003, Apyrase, BzATP, ATPγS). Data represented are mean ± SD, repeated measured one-way ANOVA with Tukey's multiple comparison test. * $p<0.05$ compared to KA. n = number of retinas. A74 = A740003. Apyr = Apyrase. KA rec = KA recovery with KA alone after drug application.

Drug	KA-Induced Ca^{2+} Response (mean ± SD)							
	rd1				wt e^-			
	KA	KA + drug	KA rec	n	KA	KA + drug	KA rec	n
A74	0.53 ± 0.04	0.41 ± 0.09*	0.56 ± 0.04	6	0.43 ± 0.04	0.40 ± 0.03	0.48 ± 0.05	5
Apyr	0.50 ±0.05	0.43 ± 0.06*	0.52 ± 0.06	7	0.42 ± 0.06	0.44 ± 0.02	0.47 ± 0.02	3
BzATP	0.46 ± 0.04	0.42 ± 0.10	0.43 ± 0.08	7	0.39 ±0.04	0.37 ± 0.06	0.42 ± 0.05	4
ATPγS	0.47 ± 0.04	0.45 ± 0.01	0.43 ± 0.01	4	0.38 ± 0.05	0.37 ±0.04	0.40 ± 0.06	4

Table 3.7. Peak KA-induced Ca^{2+} response in *rd1* GCLn with A740003 and A740003 + ATPγS. Data represented are mean ± SD, repeated measured one-way ANOVA with Tukey's multiple comparison test. * $p<0.05$ compared to KA. n = number of retinas.

	KA-Induced Ca^{2+} Response (mean ± SD)			
	KA	KA + A740003	KA + A740003 + ATPγS	n
rd1	0.51 ± 0.03	0.40 ± 0.07*	0.56 ± 0.05	5

A)

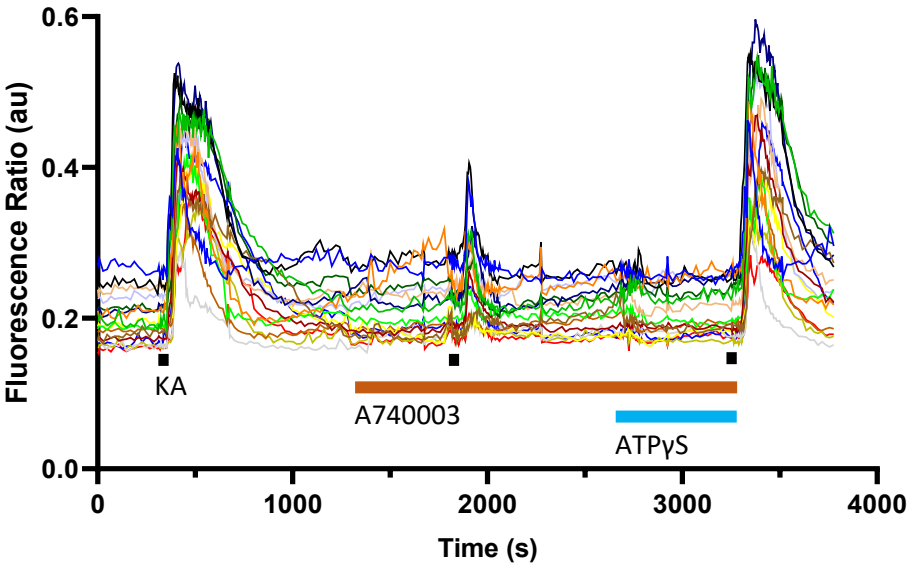
Fluorescence Ratio (au)
0.6
0.4
0.2
0.0
0
1000
2000
3000
4000
Time (s)
KA
A740003
ATPγS

B)

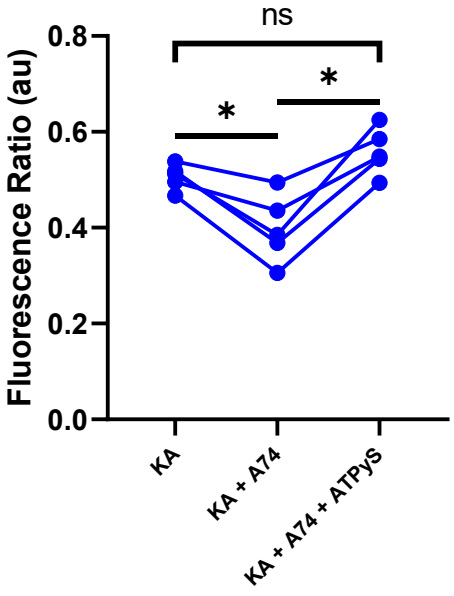
ns
*
*
Fluorescence Ratio (au)
0.8
0.6
0.4
0.2
0.0
KA
KA + A74
KA + A74 + ATPγS

Figure 3.8: Enhanced KA-induced Ca^{2+} transients are maintained in GCLn by ATP in the presence of P2X7 receptor antagonist. (A) Traces of fura-2 fluorescence ratios from 17 GCLn in an *rd1* retina over time illustrating the effect of 10 μM A740003 and 185 μM ATPγS on KA-induced Ca^{2+} transients. Black bar indicates KA, brown bar indicated A740003, blue bar indicates ATPγS. (B) Fura-2 fluorescence ratio in GCLn in *rd1* retinas treated with 50 μM KA alone (KA), in the presence of 10 μM A740003 (KA + A74) or in the presence of 10 μM A740003 and 185 μM ATPγS (KA + A74 + ATPγS). Each data point represents the averaged value from a single retina. * $p<0.05$ (repeated measures one-way ANOVA, Tukey's multiple comparison test).

Chapter 4: Discussion

Inherited retinal degenerations, including those associated with retinitis pigmentosa, have an estimated incidence of 1:2000 and are the leading cause of vision loss in people aged 15-45 years (Rattner *et al.* 1999; Hamel 2006; Krumpasky *et al.* 1999). In Canada, the prevalence of retinitis pigmentosa is somewhat less (1:4000) according to Fighting Blindness Canada. Current treatment modalities in research include gene therapy, optogenetics, cell transplantation, and electrical implant insertion (Bakondi *et al.* 2015, Tochitsky *et al.* 2016, Schwartz *et al.* 2015, Zrenner *et al.* 2011). The success of treatment depends on the stage of degeneration and viability of retinal circuitry when treatment occurs; however, many treatments are tested on late stage disease and are limited with respect to quality of vision they restore. Human clinical trials for retinitis pigmentosa treatments are ongoing across the world, but according to Fighting Blindness Canada, there is only one approved treatment for RP in the United States called Luxturna. Luxturna is a gene therapy to halt and restore some vision loss in patients with a rare RP mutation in the RPE65 gene (Darrow 2019). As RP is a family of retinal degenerative diseases caused by many known and unknown genetic mutations, there are currently limited number of successful treatment options for patients suffering from the disease.

The earliest phases of retinal degeneration are characterized by photoreceptor loss (Kolb and Gouras 1974, Marc *et al.* 2003, Kalloniatis *et al*. 2016) with later phases leading to retinal remodelling (Fariss *et al*. 200l, Marc *et al*. 2003, Jones and Marc 2005). Therefore, one strategy to restore vision in patients with retinal degeneration could be to make RGCs light sensitive, independent of upstream retinal neurons or circuitry. An underlying assumption of this approach is that RGCs will remain viable during the late

phases of retinal degeneration. Tochitsky and colleagues (2014) successfully photosensitized a population of RGCs and restored visual function in the *rd1* mouse retina, a commonly used animal model of retinal degeneration, by intraocular injection of an azobenzene "photoswitch" called DENAQ. The same group (Tochitsky *et al*. 2016) provided evidence of increased expression of P2X4r and P2X7r in *rd1* retinas and elevated levels of extracellular ATP; conditions necessary to form large conductance membrane pores that mediate DENAQ passage into OFF RGCs.

The utility of P2X4r/P2X7r pores on OFF RGCs for DENAQ loading could represent a strategy for vision restoration in people with retinal degeneration; however, the presence of P2X4r/P2X7r pores could also provide a conduit for Ca^{2+} entry and increase $[Ca^{2+}]_i$ that could alter normal RGC activity or ultimately lead to RGC death. There is evidence that P2X7r activation can lead to RGC death (Hu *et al*. 2010; Zhang *et al.* 2005). Therefore, the key objective of my thesis was to determine if the intracellular Ca^{2+} dynamics of RGCs in *rd1* mice differs from RGC in wt mice. I hypothesized that the presence of P2Xr pores on RGCs would lead to elevated resting $[Ca^{2+}]_i$ or enhanced elevations of $[Ca^{2+}]_i$ when RGCs were excited by exposure to the glutamate receptor agonist, kainic acid.

Before embarking on studies of the Ca^{2+} dynamics of RGCs in *rd1* retina, I first considered if the pathway the allows DENAQ loading (P2X4r/P2X7r pores) might also provide a conduit to specifically load the RGCs of interest with the calcium-indicator dye, fura-2.

4.1 Fura-2 Loading in rd1 Retina

Fura-2 is one of the most commonly used calcium indicator dyes. This is due, in part, to the fact that it permits ratiometric imaging: the ratio of fluorescence produced at two different excitation wavelengths corrects for differential dye loading and changes of loaded dye concentration over time (Grynkiewicz *et al.* 1985). Fura-2 (in the form of a salt) is water soluble but is not membrane permeable. The acetomethoxy ester (AM) derivative of fura-2, fura-2 AM, renders fura-2 membrane permeable and is cleaved off by endogenous esterases by hydrolysis once across the plasma membrane; this allows the fura-2 to dissolve in the aqueous cytoplasm and trapping it within the cell (Tsien 1981). Therefore, fura-2 AM has been used extensively to study $[Ca^{2+}]_i$ in cells *in vitro*. For reasons that are not clear, fura-2 AM does not load neurons well in intact adult mammalian retinal tissue preparations when applied by intraocular injection or when isolated retina is incubated in fura-2 AM solutions (Baldridge 1996). One approach to address this loading problem is to use electroporation where brief electrical currents create transient holes in the plasma membrane and allow the entry of large molecules into cells (Bonnot *et al*. 2005, Yu *et al.* 2009). A limitation of electroporation is that it unlikely loads specific subtypes of neurons and in the GCL of the retina, it loads both displaced amacrine cell and RGCs (Jeon *et al*. 1998, Daniels 2011).

As described above, Tochitsky *et al.* (2016) suggested that OFF RGCs of *rd1* retinas possess P2Xr pores that allow intracellular loading of the photoswitch molecule DENAQ. There are several reports suggesting that P2X7r pores allow the passage of fura-2 in other cell populations (Steinberg *et al*. 1987, Rassendren *et al.* 1997). I found that there was abundant fura-2 (salt) loading of GCLn in *rd1* retinas which did not occur

in wt retinas (Figure 3.2). Loading was achieved by intraocular injection of fura-2 in isolated eyes or by incubation of isolated retina in fura-2 solution. Fura-2 loading of GCLn in *rd1* retina was reported previously by Sekaran *et al.* (2003), but they used fura-2 AM (isolated retina incubation). It is possible that fura-2 AM loading is more effective in *rd1* retina than in wt, but it is also possible that sufficient fura-2 AM had been hydrolyzed generating aqueous fura-2 that could load GCLn. The extent of loading achieved by Sekaran *et al.* (2003) using fura-2 AM was not quantified but was qualitatively similar to what I achieved using fura-2 salt. Sekaran *et al.* (2003) did not identify all the types of GCLn loaded with fura-2; however, they observed light-induced increases of $[Ca^{2+}]_i$ in 2.7% of the *rd1* GCLn studied and provided evidence that, as upstream photosensitive retina was degenerated, these cells could be intrinsic photosensitive (melanopsin-containing) RGCs (ipRGCs) and GCLn that were gap junction-coupled to ipRGCs.

The loading of GCLn in *rd1* retina by fura-2 could be explained by the presence of P2Xr pores. However, I found that application of P2Xr antagonists (A740003, PPADS, or TNP-ATP), that reduced or blocked DENAQ loading (Tochitsky *et al*. 2016), had no effect on fura-2 loading of GCLn in *rd1* retinas (Figure 3.3). In fact, there was more fura-2 loading in the presence of A740003. In addition, I found that YO-PRO-1, a P2Xr-permeable nuclear dye (Virginio *et al.* 1999, Khakh *et al*. 1999) that labelled the same cells (a population of OFF RGCs) as DENAQ in *rd1* mice (Tochitsky *et al.* 2016) did not localize with the cells that loaded with fura-2 (Figure 3.4). These data suggest that the fura-2 loading of GCLn is not mediated by P2Xr pores and that fura-2 does not load the same population of GCLn in *rd1* retina (OFF RGCs) that is loaded by DENAQ or YO-PRO-1.

What mechanism might explain fura-2 loading in *rd1* retina? When under prolonged agonist activation, like certain P2Xr, transient receptor potential vanilloid 1 (TRPV1) ion channels become permeable to large cations (Man-Kyo Chung *et al.* 2008). TRPV1 channels are expressed by RGCs (Sappington *et al.* 2009) but Tochitsky *et al*. (2016) did not find an effect of TRPV1 antagonists (AMG517 and capsazepine) on DENAQ or YO-PRO-1 loading in *rd1* retina. It is possible that TRPV1 channels could be the conduit for fura-2 loading of GCLn of *rd1* retinas. Another potential mechanism of fura-2 loading of GCLn in *rd1* retina are pannexin 1 channels. Pannexin 1 channels allow entry of large dyes (Thompson *et al.* 2008) and have been shown to be expressed by RGCs (Dvoriantchikova *et al.* 2018). Another possible route for fura-2 loading are maitotoxin-activated ion channels. These channels have been studied alongside the P2X7r by Schilling *et al.* (1999) and are non-selective cation channels that, like P2X7r, can become permeable to large molecules (e.g. ethidium bromide). However, there is no research to my knowledge that has localized maitotoxin channels in the mammalian retina. Whatever the mechanism by which fura-2 loads GCLn in *rd1* retina, the enhancement of loading by the P2X7r antagonist A740003 (Figure 3.3A) might suggest the presence of P2X7r-mediated inhibition of the mechanism by which fura-2 loads certain GCLn in *rd1* retina.

The extent of fura-2 (salt) loading of GCLn in *rd1* retina by intraocular injection was comparable with the loading in wt achieved by electroporation following intraocular injection, and fura-2 loading in *rd1* retina was not enhanced by electroporation following intraocular injection (Figure 3.2). This result was not predicted as the labelling produced by electroporation was expected to be less discriminating than the loading achieved by intraocular injection of fura-2. It is possible that GCLn loaded with fura-2 in *rd1* retina by

intraocular injection alone are the same, or very similar, to the cells loaded by electroporation in *rd1* or even wt retinas. I also observed that GCLn loaded with fura-2 in *rd1* retinas did not localize with YO-PRO-1 (presumably labelling the OFF RGCs described by Tochitsky *et al.* 2016). It would be interesting to determine if fura-2 loaded GCLn in electroporated *rd1* or wt retinas are also labelled by YO-PRO-1. Why the electroporation loading of fura-2 might preferentially load the same GCLn loaded by the intraocular injection of fura-2 alone and is distinct from those labelled with YO-PRO-1 in *rd1* retinas is not clear.

The GCL of the mouse retina contains roughly equal numbers of RGCs and displaced amacrine cells (Jeon *et al.* 1998). I did not determine which type of neurons in the GCL were loaded by fura-2, meaning that the population of GCLn loaded with fura-2 could represent a mixture of both RGCs and amacrine cells. A previous study of fura-2 loading achieved by electroporation in wt retinas was performed where RGCs were first labelled by rhodamine dextran applied to the superior colliculus, and suggested a slight preference for RGC loading; 66% of fura-2-loaded cells were RGCs (Daniels 2011). Nonetheless, electroporation results in both displaced amacrine cell and RGC loading with fura-2. Given the similarity of fura-2 loading in *rd1* retinas (intraocular injection alone) and *rd1* and wt retinas subject to electroporation (intraocular injection followed by electroporation), the results suggests that in each case the GCLn with fura-2 are a mixed population of displaced amacrine cells and RGCs. To determine definitively which GCLn load with fura-2 in the *rd1* retina is difficult, as fura-2 is not preserved in cells following fixation. Therefore, it is not possible to use selective immunohistochemical markers for RGCs, such as RNA-binding protein with multiple splicing (RBPMS; Rodriguez *et al.*

2014) or displaced amacrine cells loaded with dyes (Perez De Sevilla Müller *et al*. 2007) to assess co-localization with fura-2. Which GCLn in *rd1* retinas load with fura-2 could be determined by crossing *rd1* mice with transgenic mice that express a fluorescent protein in specific types of GCLn such as the Thy1-GCaMP3 transgenic mouse line. It expresses genetically encoded GCaMP3 fluorescence under control of the Thy1 promoter (Chen *et al*. 2012) and in retina has been found to be preferentially expressed in RGCs (Blandford *et al.* 2019).

4.2 Calcium Dynamics

4.2.1 Baseline $[Ca^{2+}]_i$

Although the mechanism that mediates fura-2 loading of GCLn in *rd1* retinas was not clear, I wondered if this might also represent a conduit for Ca^{2+} entry that could increase baseline $[Ca^{2+}]_i$. Intracellular Ca^{2+} is an important second messenger and, therefore, $[Ca^{2+}]_i$ is closely regulated, with cells constantly working to maintain $[Ca^{2+}]_i$ concentration by efflux through the action of Ca^{2+} ATPase pumps or storage within internal organelles (Berridge *et al*. 2000). Typically $[Ca^{2+}]_i$ is maintained at < 200 nM, creating a 10,000-fold concentration gradient between cellular cytosolic and extracellular space (Carafoli *et al*. 2001). If control of the $[Ca^{2+}]_i$ fails, prolonged elevation of $[Ca^{2+}]_i$ has been shown to lead to cellular death (Orrenius and Nicorera 1994, Carafoli 2004). Contrary to our hypothesis, there was no difference in the tonic baseline $[Ca^{2+}]_i$ between *rd1* and wt GCLn, nor a difference between retinas where fura-2 was loaded by incubation alone or by electroporation (Figure 3.5). Therefore, the mechanism that mediates fura-2-loading of some *rd1* GCLn either does not permit Ca^{2+} influx or the *rd1*

GCLn are able to maintain baseline Ca^{2+} at levels comparable to wt GCLn. With respect to the latter, there is evidence that GCLn possess several different Ca^{2+}-binding proteins (Wässle *et al.* 1998; Haeseleer *et al.* 2000; Ghosh *et al.* 2004) that could effectively buffer $[Ca^{2+}]_i$ (Falke *et al.* 1994; Schäfer and Heizmann 1996; Schwaller *et al*. 2002).

As described above (Section 4.1), YO-PRO-1 did not load the same GCLn in *rd1* retinas that were loaded with fura-2. Nonetheless, I wondered if baseline $[Ca^{2+}]_i$ in *rd1* GCLn would be affected by P2Xr modulation. Would baseline $[Ca^{2+}]_i$ be reduced by P2X7r antagonism with A740003 or by extracellular ATP degradation with the apyrase, and would it be elevated with the P2X agonist BzATP or the non-hydrolysable analogue of ATP, ATPγS? Baseline $[Ca^{2+}]_i$ in *rd1* GCLn was not affected by any of the purinergic drugs used (Figure 3.5B-E). These findings support the conclusion from my studies using YO-PRO-1, that P2X7r are not located on fura-2-loaded *rd1* GCLn. Similar findings occurred in wt GCLn; there was no change in baseline $[Ca^{2+}]_i$ after A740003, apyrase, or BzATP (Figure 3.5B-D) but ATPγS did cause an increase in baseline $[Ca^{2+}]_i$ (Figure 3.5E).

Previous studies of wt rodent retina have suggested that BzATP increases $[Ca^{2+}]_i$ in RGCs (Zhang *et al.* 2005; Hu *et al.* 2010). However, these experiments were done using RGCs isolated (*in vitro*) from neonatal retinas, conditions that might favour increased expression of P2Xr. It is possible that the effect I observed with ATPγS reflects some degree of P2Xr expression in wt retina, but this would not explain why BzATP was without effect. My study is the first using intact retina preparations to study calcium dynamics of GCLn, although it is worth noting that one study using intact rat retina did not find YO-PRO-1 loading of GCLn in wt retina during even prolonged (10 min)

exposure to BzATP (Innocenti *et al*. 2004) and this result is also what was reported by Tochitsky *et al.* (2016).

In their studies of *rd1* retina, Tochitsky *et al.* (2016) concluded that there is increased extracellular ATP and P2Xr up-regulation and this permits the loading of the photoswitch DENAQ or YO-PRO-1. My results do not provide evidence for increased P2Xr in GCLn from *rd1* retinas in that baseline $[Ca^{2+}]_i$ was not different from that in wt retinas and that P2Xr drugs did not alter *rd1* GCLn $[Ca^{2+}]_i$. However, as described above, the fura-2 loaded GCLn I studied appear to be a different population of GCLn than those studied by Tochitsky *et al*. (2016) that could be loaded by YO-PRO-1.

Collectively, these data suggest that the resting $[Ca^{2+}]_i$ in *rd1* GCLn is not affected by P2Xr manipulation and does not support the original hypothesis that GCLn from *rd1* retinas have altered purinergic sensitivity relative to wt.

4.2.2 KA-induced Ca^{2+} Response and Modulation

Another objective of this thesis was to assess the effect of kainic acid (KA), an ionotropic glutamate receptor agonist, on fura-2-loaded GCLn of the *rd1* retinas in comparison with wt. Although the conduit by which fura-2 loads GCLn in *rd1* retina did not affect baseline $[Ca^{2+}]_i$, might it alter GCLn Ca^{2+} dynamics when the cells are stimulated by KA application? Kainic acid is a slowly desensitizing agonist of ionotropic AMPA receptors (the predominant glutamate receptor type of GCLn) and activation facilitates a non-selective cation conductance (Mayer and Westbrook 1987) that would lead to GCLn depolarization. The depolarization causes voltage-gated cation channels to

open and Ca^{2+} influx into the cell. When applied to the retina, KA caused a transient increase of fura-2 ratio in GCLn (Figure 3.6A-C). In my experiments, the change in $[Ca^{2+}]_i$ produced by KA was documented as the peak of the transient increase of fura-2 ratio, referred to as the KA-induced Ca^{2+} response.

The first series of experiments showed that the peak KA-induced Ca^{2+} response was greater in *rd1* retinas compared to wt (Figure 3.7A). The increased KA-induced Ca^{2+} response was observed in *rd1* retina loaded with fura-2 either without electroporation (intravitreal injection of fura-2 alone) or after electroporation. This was done to assess the effect of electroporation on *rd1* retinas, as it was necessary for substantial fura-2 loading in wt retinas. As electroporation did not alter the peak KA-induced Ca^{2+} responses of *rd1* retinas, subsequent experiments were performed using *rd1* retinas loaded with fura-2 without electroporation and wt retinas loaded using electroporation.

To determine if P2Xr were involved in the enhanced response of *rd1* GCLn to KA, the P2X7r antagonist A740003 or the ATP-degrading enzyme apyrase were applied simultaneously with KA. The enhanced KA-induced Ca^{2+} response was significantly reduced by both A740003 and apyrase in *rd1* retinas with no effect on the wt retinas (Figure 3.7B, C). These data suggest a role for ATP and P2X7r in the enhanced KA-induced Ca^{2+} response in fura-2-loaded *rd1* GCLn. A possible explanation for the enhancement of the KA-induced Ca^{2+} response in *rd1* retinas is that ATP is released during KA application and the elevated extracellular ATP activates GCLn P2X7r thereby enhancing Ca^{2+} influx, directly through P2X7r or indirectly by further activation of voltage-gated Ca^{2+} channels. However, this would require that P2X7r expression is increased in *rd1* GCLn. Although this is exactly the change suggested by Tochitsky *et al.*

(2016), recall that the cell types they studied (a population of OFF RGCs that load with YO-PRO-1) do not appear to be the same cells I studied (loaded by fura-2 but not YO-PRO-1). Furthermore, if P2X7r are upregulated in the population of GCLn cells I studied, it would have been predicted that P2X7r agonists (BzATP and ATPγS) should have altered baseline $[Ca^{2+}]_i$. In addition, when applied in the presence of BzATP or ATPγS, KA-induced Ca^{2+} response in *rd1* retinas were not (or not effectively) affected (Figure 3.7D, E).

If KA increases ATP release in *rd1* retina and leads to enhanced GCLn Ca^{2+} dynamics by acting on the fura-2 loaded GCLn P2X7r, then the P2X7r antagonist A740003 should not only reduce the response to KA but should also block the effect of a subsequent treatment with ATPγS. However, I found that ATPγS enhanced the KA-induced responses in the presence of A740003 (Figure 3.8). These results suggest that whilst antagonism of P2X7r reduces the enhancement of KA-induced Ca^{2+} responses, the mechanism is not simply explained by enhanced release of ATP acting on the fura-2 labelled GCLn P2X7r.

How could the P2X7r-specific antagonist A740003 affect the KA-response in the fura-2 labelled GCLn in *rd1* retina? One possibility is that in the *rd1* retina P2X7r are expressed on another cell population, not the GCLn loaded with fura-2, and these P2X7r allow the efflux of ATP, efflux that is increased by KA. Several studies have shown that P2X7r pores can mediate ATP release that affects other cell types (Ohshima *et al.* 2010, Suadicani *et al*. 2006, Pellegatti *et al.* 2011). The increased extracellular ATP could then act on P2 receptors on the fura-2 loaded GCLn to enhance the KA-induced Ca^{2+} response. If this model is true, P2X7r antagonists (like A740003) would not block the

effect of ATP on the fura-2 loaded GCLn themselves, but instead block ATP efflux from the P2X7r-containing cells. In support of this idea I found that even though the KA-induced Ca^{2+} response in *rd1* retinas was reduced by A740003, the KA-induced response was increased by treatment with ATPγS (a general P2r and subtype agonist) (Figure 3.8). This suggests the enhancement is not due to the action of ATP on P2X7r but could be due to other P2r on the fura-2 loaded GCLn in *rd1* retinas. This result may also explain why neither BzATP or ATPγS enhanced KA-induced Ca^{2+} responses (Figure 3.7D, E). If, in *rd1* retinas, KA application results in ATP release via P2X7r pores, the level of ATP acting on GCLn could be saturating and, under these conditions, BzATP or ATPγS would have no effect.

If, as suggested above, P2r (but not P2X7r) on fura-2 loaded GCLn in *rd1* retinas are affected by ATP released via P2X7r pores on other cell types, why did ATPγS not affect baseline $[Ca^{2+}]_i$? This suggests that the effect of ATP on the $[Ca^{2+}]_i$ in these GCLn is not due to the additive effect of P2r-induced changes of $[Ca^{2+}]_i$ (that should also alter baseline $[Ca^{2+}]_i$) and KA-induced changes of $[Ca^{2+}]_i$ (additive effect), but requires an enhancement of the effect of KA on these cells (synergistic effect). That is, KA treatment not only enhances the release of ATP, but the ATP then acts to modulate (enhance) the effect of KA on GCLn $[Ca^{2+}]_i$.

The interpretation of the results provided above may imply that the effect of KA was selective for the GCLn studied (those that load with fura-2). This is, of course, not correct; KA applied by superfusion could target AMPA receptors on any retinal cell (neuron or glia) type. Therefore, the KA-induced Ca^{2+} response in GCLn represents the direct effect on GCLn and the indirect effect on other cell types that could influence,

either positively (excitation) or negatively (inhibition), the GCLn being studied. Consequently, when interpreting the increase of the KA-induced Ca^{2+} response in GCLn in *rd1* retinas, compared to wt retinas, this could indicate a direct enhancement of the effect of KA on GCLn, an increase in excitatory input to GCLn or a decrease in inhibitory input. Furthermore, the fact that the P2X7r antagonist A740003 reduces the enhanced (relative to wt) KA-induced Ca^{2+} response in *rd1* retinas could be explained by the presence of P2X7r on GCLn or the presence of P2X7r on cells controlling (indirectly) excitatory or inhibitory input to GCLn. The fact that the enhanced KA-induced Ca^{2+} response, reduced by A740003, was restored by ATPγS suggests that the enhancement is not due to the action of ATP on P2X7r, at any of the potential targets (GCLn directly or indirectly, via excitatory or inhibitory inputs to GCLn) but could be due to other P2r. A possible explanation for the effect of A740003 is that, in *rd1* retina, there are cell types that possess P2X7r pores that allow the efflux of ATP that then can affect KA-induced Ca^{2+} responses in fura-2-loaded GCLn either directly or indirectly.

My results are broadly consistent with the conclusion made by Tochitsky *et al.* (2016) that extracellular ATP is elevated in *rd1* retinas compared to wt retinas. In their study, the effect of such elevated ATP was to promote the formation of P2X7r pores that permitted the loading of OFF RGCs with YO-PRO-1 and the photoswitch (DENAQ), thereby restoring light responses in these cells and explaining vision restoration (Tochitsky *et al*. 2014). From my work, I suggest that ATP release via P2X7r pores (increased in *rd1* retina relative to wt) is enhanced by KA treatment leading to activation of P2 receptors, on those GCLn that loaded with fura-2. A key question is what cell type would be a good candidate as the source of ATP released via P2X7r pores? In the retina,

the P2X7r is normally expressed by many cell populations including photoreceptors, amacrine cells, RGCs and Müller cells (Brandle *et al.* 1998, Pannicke *et al.* 2000, Wheeler-Schilling *et al.* 2001, Puthussery and Fletcher 2009). Although ATP released from photoreceptors seems unlikely to reach GCLn, the amacrine cells, Müller cells or RGCs would all be capable of releasing ATP that could act on fura-2-loaded GCLn. An interesting possibility is that the OFF RGCs identified by Tochitsky *et al.* (2016), with elevated P2Xr pores, could be the source of ATP that could act on the fura-2 loaded GCLn identified in my study.

4.3 Future Directions

4.3.1 Fura-2 GCLn Loading

The data presented suggest that the fura-2 loading in *rd1* GCLn was not mediated by P2Xr and further study is needed to determine which types of GCLn are loaded with fura-2 and the mechanism involved. As described above, it would be beneficial to determine if TRPV1, pannexin 1 or maitotoxin channels mediate fura-2 loading by assessing the effect of specific blockers on fura-2 loading in *rd1* retinas.

Another experiment that could be undertaken to identify the fura-2 labelled GCLn could be to cross the Thy1-GCaMP3 transgenic mouse line with the *rd1* mouse line. The Thy1-GCaMP3 model expresses genetically encoded GCaMP3 fluorescence under control of the Thy1 promoter (Chen *et al*. 2012) and in retina has been found to be preferentially expressed in RGCs (Blandford *et al.* 2019). Colocalization experiments could be performed to determine whether the fura-2 loaded cells were amacrine cells vs. RGCs. Another useful transgenic mouse model could be the P2X7-EGFP transgenic

mouse (Garcia-Huerta *et al*. 2012). Although to my knowledge there has been no research using this transgenic line to study the retina, in principle this line, if crossed with an *rd1* line, could be used to examine P2X7 receptor distribution in *rd1* retina.

4.3.2 KA-induced Calcium Dynamics

My results indicated that KA-induced Ca^{2+} responses in fura-2 loaded GCLn were increased in *rd1* retinas compared to retina from wt animals. Although this effect was reduced by treatment with the P2X7 antagonist A740003 or by enzymatic degradation of exogenous ATP by apyrase, additional experiments suggested that the increased KA-induced Ca^{2+} response in *rd1* retina could not be explained by ATP acting on P2X7 receptors expressed by the GCLn that were loaded with fura-2. If this were the case then ATPγS, applied in the presence of A740003, should have had no effect on KA-induced Ca^{2+} responses. Instead, ATPγS restored the enhancement of the KA-induced Ca^{2+} response. I proposed a possible explanation, that in *rd1* retinas KA promotes the release of ATP through P2X7r from an unknown population of cells (neurons or glia) that then acts on P2 receptors on the GCLn, or on cells pre-synaptic to GCLn, thereby adding to or enhancing the effect of KA on the fura-2 loaded GCLn. The effect of the P2X7 antagonist A740003 could be explained by blockade of P2X7 pores that have been shown to permit the release of ATP, but the effect of ATP on fura-2-loaded GCLn would not be due to P2X7r because ATPγS was able to restore the enhancement of KA-induced Ca^{2+} responses in the presence of A740003. This means that the action of ATP on fura-2-loaded GCLn would be mediated by some other type(s) of P2r, P2Xr or P2Yr. Therefore, an obvious future direction would be to determine if other P2r antagonists reduce the

effect of KA on fura-2 loaded GCLn. This is not as straight-forward as might be assumed. Several P2r antagonists (like the non-selective antagonist, PPADs, and the P2Xr antagonist, TNP-ATP, both used by Tochitsky *et al.* (2016) in their study) interfere with fura-2 fluorescence and, therefore, could not be used. Therefore, drugs need to be selected with care to ensure they do not interfere with fura-2 fluorescence. A possible solution would be to employ the Thy1-GCaMP3 transgenic mouse line (described above) crossed with the *rd1* mouse line. This crossed line could be used to identify the fura-2 loaded GCLn but then calcium-imaging performed using GCaMP3, the fluorescence of which might not be affected by P2r antagonists. Such a *rd1*/Thy1-GCaMP3 line would also allow GCaMP3 calcium imaging of fura-2-loaded GCLn to be compared to GCLn that do not load with fura-2, presumably containing the population of OFF RGCs that load with YO-PRO-1 and were studied by Tochitsky *et al.* (2016).

The other major component of the model I have proposed is that, in *rd1* retina, ATP is released via P2X7r pores that can be blocked by P2X7r antagonists. In fact, I only tested one antagonist (A740003) and it would probably be important to test additional P2X7r antagonists, taking into consideration the same limitations imposed by drugs that interfere with fura-2 fluorescence. An *rd1*/Thy1-GCaMP3 mouse line would again be useful to deal with this limitation. In addition, it would be interesting to study an *rd1*/P2X7r knockout cross (P2X7r knockout mice are commercially available, e.g. the $P2rx7^{tm1Gab}$ mouse available from the Jackson Laboratory). It would also be ideal to demonstrate ATP release from a retinal cell type via P2X7r pores. Such release has been demonstrated from several different types of cells (Ohshima *et al.* 2010, Suadicani *et al*. 2006, Pellegatti *et al.* 2011) but in all cases these studies were done using isolated cells

(*in vitro*) with ATP assayed after release into cell culture media. This does not preclude the study of possible retinal cell candidates (mentioned above) that could be the source of ATP release, but the procedures (such as assays) required to produce such *in vitro* preparations could be a potential confound. Another useful approach would be to study specific cell types (neurons and glia) in the *rd1* retina to determine which might show increased expression of P2X7r. Presumably some of these cells are those that load with YO-PRO-1 (Tochitsky *et al*. 2016). This could be done *in vitro*, subject to the same limitation mentioned above, or *in situ* by calcium-imaging experiments, with targeted expression of loading with Ca^{2+}-sensitive dyes or targeted expression Ca^{2+}-sensitive proteins. Alternatively, electrophysiological studies of individual cells in *rd1* retina could help identify which types have altered P2X7r expression. However, for such studies to have context, data from wt retinas would also be required.

My experiments did not distinguish the potential source of ATP in the *rd1* retina and also did not indicate which cells are the actual target of ATP that ultimately leads to increased KA-induced Ca^{2+} responses. This could also be studied further by calcium-imaging or electrophysiology experiments (*in vitro* or *in situ*) to determine which cells from *rd1* retina show altered P2r (including but not limited to P2X7r) activity. Again, for such experiments to meaningful would require data from wt retinas.

4.4 Conclusions

There has been abundant research that aims to restore vision in degenerated retinas through methods such as gene therapy, photoreceptor and retinal pigmented epithelium cell transplantation, and electrical implants (Bakondi *et al.* 2015, Schwartz *et al.* 2015,

Zrenner *et al.* 2011). However, the status and continued viability of the degenerated retinal circuitry must be taken into consideration when determining the likely success of these treatments (Marc *et al.* 2003). My results provide additional information that in an animal model of retinal degeneration (the *rd1* mouse) there is altered purine signalling. Not only might normal retinal processing be affected by abnormal purine signalling, increased $[Ca^{2+}]_i$ in GCLn could, overtime, lead to cell death. These data add to observations that there is more complexity in the *rd1* model of retinal degeneration than just photoreceptor loss and, therefore, efforts to recover photosensitivity following degeneration in the *rd1* mouse by targeting the outer retina alone may not be sufficient. The purine signalling pathway is thus another altered feature that will need to be taken into consideration as part of efforts to restore vision in patients with retinal degeneration.

References

And, Y. K., & Ebrey, T. G. (1986). Recent progress in vertebrate photoreception. *Photochemistry and Photobiology*, *44*(6), 809–817.

Arshavsky, V. Y., Lamb, T. D., & Pugh, E. N. (2002). G proteins and phototransduction. *Annual Review of Physiology*, *64*(Journal Article), 153.

Ashmore, J. F., & Copenhagen, D. R. (1980). Different postsynaptic events in two types of retinal bipolar cell. *Nature*, *288*(5786), 84–86.

Bakondi, B., Lv, W., Lu, B., Jones, M. K., Tsai, Y., Kim, K. J., Levy, R., Akhtar, A. A., Breunig, J. J., Svendsen, C. N., & Wang, S. (2015). In vivo CRISPR/ Cas9 gene editing corrects retinal dystrophy in the S334ter- 3 rat model of autosomal dominant retinitis pigmentosa. *Molecular Therapy*, *24*(3).

Bartlett, R., Stokes, L., & Sluyter, R. (2014). The P2X7 receptor channel: recent developments and the use of P2X7 antagonists in models of disease. *Pharmacological Reviews*, *66*(3), 638–675.

Baldridge, W. H. (1996). Optical recordings of the effects of cholinergic ligands on neurons in the ganglion cell layer of mammalian retina. *The Journal of Neuroscience : The Official Journal of the Society for Neuroscience*, *16*(16), 5060–5072.

Berridge, M. J., Lipp, P., & Bootman, M. D. (2000). The versatility and universality of calcium signalling. *Nature Reviews Molecular Cell Biology*, *1*(1), 11.

Berson, E. L., Gouras, P., & Gunkel, R. D. (1968). Rod responses in retinitis pigmentosa, dominantly inherited. *Archives of Ophthalmology (Chicago, Ill.: 1960)*, *80*(1), 58.

Blackshaw, L. A., Page, A. J., & Young, R. L. (2011). Metabotropic glutamate receptors as novel therapeutic targets on visceral sensory pathways. *Frontiers in Neuroscience*, *5*(Journal Article), 40–40.

Blandford, S. N., Hooper, M. L., Yabana, T., Chauhan, B. C., Baldridge, W. H., & Farrell, S. R. M. (2019). Retinal characterization of the Thy1-GCaMP3 transgenic mouse line after optic nerve transection. *Investigative Ophthalmology & Visual Science*, *60*(1), 183–191.

Bleakman, D., & Lodge, D. (1998). Neuropharmacology of AMPA and kainate receptors. *Neuropharmacology*, *37*(10–11), 1187–1204.

Bloomfield, S. A., & Dowling, J. E. (1985). Roles of aspartate and glutamate in synaptic transmission in rabbit retina. II. inner plexiform layer. *Journal of Neurophysiology*, *53*(3), 714.

Bonnot, A., Mentis, G. Z., Skoch, J., & O'Donovan, M., J. (2005). Electroporation loading of calcium- sensitive dyes into the CNS. *Journal of Neurophysiology*, *93*(3), 1793–1808.

Bowes, C., Li, T., Danciger, M., Baxter, L. C., Applebury, M. L., & Farber, D. B. (1990). Retinal degeneration in the rd mouse is caused by a defect in the β subunit of rod cGMP- phosphodiesterase. *Nature*, *347*(6294), 677.

Boycott, B. B., Dowling, J. E., & Kolb, H. (1969). Organization of the primate retina: light microscopy. *Philosophical Transactions of the Royal Society of London.Series B, Biological Sciences (1934-1990)*, *255*(799), 109–184.

Brändle, U., Kohler, K., & Wheeler-Schilling, T. (1998a). Expression of the P2X 7-receptor subunit in neurons of the rat retina. *Molecular Brain Research*, *62*(1), 106–109.

Bringmann, A., Pannicke, T., Grosche, J., Francke, M., Wiedemann, P., Skatchkov, S. N., Osborne, N. N., & Reichenbach, A. (2006). Müller cells in the healthy and diseased retina. *Progress in Retinal and Eye Research*, *25*(4), 397–424.

Burnstock, G., & Knight, G. E. (2004). Cellular distribution and functions of P2 receptor subtypes in different systems. *International Review of Cytology*, *240*(Journal Article), 31.

Carafoli, E. (2004). Calcium- mediated cellular signals: a story of failures. *Trends in Biochemical Sciences*, *29*(7), 371–379.

Carafoli, E., Santella, L., Branca, D., & Brini, M. (2001). Generation, control, and processing of cellular calcium signals. *Critical Reviews in Biochemistry and Molecular Biology*, *36*(2), 107–260.

Carter-Dawson, L., Lavail, M. M., & Sidman, R. L. (1978). Differential effect of the rd mutation on rods and cones in the mouse retina. *Investigative Ophthalmology & Visual Science*, *17*(6), 489–498.

Cheers, C., & McKenzie, I. F. (1978). Resistance and susceptibility of mice to bacterial infection: genetics of listeriosis. *Infection and Immunity*, *19*(3), 755.

Chen, Q., Cichon, J., Wang, W., Qiu, L., Lee, S.-J. r, Campbell, N. r, Destefino, N., Goard, M. j, Fu, Z., Yasuda, R., Looger, L. l, Arenkiel, B. r, Gan, W.-B., & Feng, G. (2012). Imaging neural activity using Thy1- GCaMP transgenic mice. *Neuron*, *76*(2), 297–308.

Cideciyan, A. V., & Jacobson, S. G. (1993). Negative electroretinograms in retinitis pigmentosa. *Investigative Ophthalmology & Visual Science*, *34*(12), 3253.

Coddou, C., Yan, Z., Obsil, T., Huidobro-Toro, J., & Stojilkovic, S. S. (2011). Activation and regulation of purinergic P2X receptor channels. *Pharmacological Reviews*, *63*(3), 641–683.

Collingridge, G. L., & Lester, R. A. (1989). Excitatory amino acid receptors in the vertebrate central nervous system. *Pharmacological Reviews*, *41*(2), 143–210.

Daniels, B. (2011). *Modulation of ionotropic glutamate receptors in retinal neurons by the amino acid D-serine*. *Generic*.

Daniels, B. A., & Baldridge, W. H. (2010). D- serine enhancement of NMDA receptor-mediated calcium increases in rat retinal ganglion cells. *Journal of Neurochemistry*, *112*(5), 1180–1189.

Darrow, J. J. (2019). Luxturna: FDA documents reveal the value of a costly gene therapy. *Drug Discovery Today*, *24*(4), 949–954.

Davies, J., & Watkins, J. (1979). Selective antagonism of amino acid- induced and synaptic excitation in the cat spinal cord. *Journal of Physiology (London)*, *297*(1), 621–635.

Di Virgilio, F. (1995). The P2Z purinoceptor: An intriguing role in immunity, inflammation and cell death. *Immunology Today*, *16*(11), 524–528.

Drury, A. N., & Szent-Györgyi, A. (1929). The physiological activity of adenine compounds with especial reference to their action upon the mammalian heart. *The Journal of Physiology*, *68*(3), 213.

Duncan, J. L., Pierce, E. A., Laster, A. M., Daiger, S. P., Birch, D. G., Ash, J. D., Iannaccone, A., Flannery, J. G., Sahel, J. A., Zack, D. J., & Zarbin, M. A. (2018). Inherited retinal degenerations: current landscape and knowledge gaps. *Translational Vision Science & Technology*, *7*(4), 6.

Dvoriantchikova, G., Pronin, A., Kurtenbach, S., Toychiev, A., Chou, T.-H., Yee, C. W., Prindeville, B., Tayou, J., Porciatti, V., Sagdullaev, B. T., Slepak, V. Z., & Shestopalov, V. I. (2018). Pannexin 1 sustains the electrophysiological responsiveness of retinal ganglion cells. *Scientific Reports*, *8*(1), 5797–5797.

Eisenstein, T. K., Deakins, L. W., Killar, L., Saluk, P. H., & Sultzer, B. M. (1982). Dissociation of innate susceptibility to Salmonella infection and endotoxin responsiveness in C3HeB/FeJ mice and other strains in the C3H lineage. *Infection and Immunity*, *36*(2), 696.

Falke, J. J., Drake, S. K., Hazard, A. L., & Peersen, O. B. (1994). Molecular tuning of ion binding to calcium signaling proteins. *Quarterly Reviews of Biophysics*, *27*(3), 219–290.

Farber, D. B., & Lolley, R. N. (1976). Enzymic basis for cyclic GMP accumulation in degenerative photoreceptor cells of mouse retina. *Journal of Cyclic Nucleotide Research*, *2*(3), 139–148.

Fariss, R. N., Li, Z. Y., & Milam, A. H. (2000). Abnormalities in rod photoreceptors, amacrine cells, and horizontal cells in human retinas with retinitis pigmentosa. *American Journal of Ophthalmology*, *129*(2), 215–223.

Ferrari, D., Los, M., Bauer, M. K. A., Vandenabeele, P., Wesselborg, S., & Schulze - Osthoff, K. (1999). P2Z purinoreceptor ligation induces activation of caspases with distinct roles in apoptotic and necrotic alterations of cell death. *FEBS Letters*, *447*(1), 71–75.

Ferrari, S., Di Iorio, E., Barbaro, V., Ponzin, D., Sorrentino, F., & Parmeggiani, F. (2011). Retinitis pigmentosa: genes and disease mechanisms. *Current Genomics*, *12*(4), 238–249.

Fischer, W., & Krügel, U. (2007). P2Y receptors: focus on structural, pharmacological and functional aspects in the brain. *Current Medicinal Chemistry*, *14*(23), 2429–2455.

Gao, F., Pang, J.-J., & Wu, S. M. (2013). Sign-preserving and sign-inverting synaptic interactions between rod and cone photoreceptors in the dark-adapted retina. *The Journal of Physiology*, *591*(22), 5711–5726.

Garcia-Huerta, P., Díaz-Hernandez, M., Delicado, E. G., Pimentel-Santillana, M., Miras-Portugal, M., & Gómez-Villafuertes, R. (2012). The specificity protein factor Sp1 mediates transcriptional regulation of P2X7 receptors in the nervous system. *The Journal of Biological Chemistry*, *287*(53), 44628–44644.

Ghosh, K. K., Bujan, S., Haverkamp, S., Feigenspan, A., & Wässle, H. (2004). Types of bipolar cells in the mouse retina. *Journal of Comparative Neurology*, *469*(1), 70–82.

Grover, S., Fishman, G. A., & Brown, J. (1998). Patterns of visual field progression in patients with retinitis pigmentosa. *Ophthalmology*, *105*(6), 1069–1075.

Grynkiewicz, G., Poenie, M., & Tsien, R. Y. (1985). A new generation of Ca^{2+} indicators with greatly improved fluorescence properties. *The Journal of Biological Chemistry*, *260*(6), 3440–3450.

Haeseleer, F., Sokal, I., Verlinde, C. L., Erdjument-Bromage, H., Tempst, P., Pronin, A. N., Benovic, J. L., Fariss, R. N., & Palczewski, K. (2000). Five members of a novel Ca(2+)-binding protein (CABP) subfamily with similarity to calmodulin. *The Journal of Biological Chemistry*, *275*(2), 1247–1260.

Hagins, W. A., Penn, R. D., & Yoshikami, S. (1970). Dark current and photocurrent in retinal rods. *Biophysical Journal*, *10*(5), 380–412.

Hamel, C. (2006). Retinitis pigmentosa. *Orphanet Journal of Rare Diseases*, *1*(Generic), 40–40.

Hartline, H. K. (1938). The response of single optic nerve fibers of the vertebrate eye to illumination of the retina. *American Journal of Physiology*, *121*(Journal Article), 400–415.

Haverkamp, S., Grünert, U., & Wässle, H. (2000). The cone pedicle, a complex synapse in the retina. *Neuron*, *27*(1), 85–95.

Heston, W. E., & Vlahakis, G. (1971). Mammary tumors, plaques, and hyperplastic alveolar nodules in various combinations of mouse inbred strains and the different lines of the mammary tumor virus. *International Journal of Cancer*, *7*(1), 141–148.

Hopkins, J. M., & Boycott, B. B. (1997). The cone synapses of cone bipolar cells of primate retina. *Journal of Neurocytology*, *26*(5), 313–325.

Hu, H., Lu, W., Zhang, M., Zhang, X., Argall, A. J., Patel, S., Lee, G. E., Kim, Y.-C., Jacobson, K. A., Laties, A. M., & Mitchell, C. H. (2010). Stimulation of the P2X 7 receptor kills rat retinal ganglion cells in vivo. *Experimental Eye Research*, *91*(3), 425–432.

Idzko, M., Ferrari, D., Riegel, A.-K., & Eltzschig, H. K. (2014). Extracellular nucleotide and nucleoside signaling in vascular and blood disease. *Blood*, *124*(7), 1029–1037.

Innocenti, B., Pfeiffer, S., Zrenner, E., Kohler, K., & Guenther, E. (2004). ATP-induced non-neuronal cell permeabilization in the rat inner retina. *Journal of Neuroscience*, *24*(39), 8577–8583.

Jeon, C. J., Strettoi, E., & Masland, R. H. (1998). The major cell populations of the mouse retina. *The Journal of Neuroscience : The Official Journal of the Society for Neuroscience*, *18*(21), 8936–8946.

Jiang, L.-H., Baldwin, J. M., Roger, S., & Baldwin, S. A. (2013). Insights into the molecular mechanisms underlying mammalian P2X7 receptor functions and contributions in diseases, revealed by structural modeling and single nucleotide polymorphisms. *Frontiers in Pharmacology*, *4*(Journal Article), 55.

Jones, B. W., & Marc, R. E. (2005). Retinal remodeling during retinal degeneration. *Experimental Eye Research*, *81*(2), 123–137.

Kalloniatis, M., Nivison-Smith, L., Chua, J., Acosta, M. L., & Fletcher, E. L. (2016). Using the rd1 mouse to understand functional and anatomical retinal remodelling and treatment implications in retinitis pigmentosa: a review. *Experimental Eye Research*, *150*(Journal Article), 106–121.

Khakh, B. S., Bao, X. R., Labarca, C., & Lester, H. A. (1999). Neuronal P2X transmitter-gated cation channels change their ion selectivity in seconds. *Nature Neuroscience*, *2*(4), 322.

Khakh, B. S., & Burnstock, G. (2009). The double life of ATP. *Scientific American*, *301*(6), 84.

Kolb, H., & Gouras, P. (1974). Electron microscopic observations of human retinitis pigmentosa, dominantly inherited. *Investigative Ophthalmology*, *13*(7), 487–498.

Krumpaszky, H. G., Lüdtke, R., Mickler, A., Klauss, V., & Selbmann, H. K. (1999). Blindness incidence in Germany. *Ophthalmologica*, *213*(3), 176–182.

Kulkarni, M., Trifunović, D., Schubert, T., Euler, T., & Paquet-Durand, F. (2016). Calcium dynamics change in degenerating cone photoreceptors. *Human Molecular Genetics*, *25*(17), 3729–3740.

Lenertz, L., Gavala, M., Zhu, Y., & Bertics, P. (2011). Transcriptional control mechanisms associated with the nucleotide receptor P2X7, a critical regulator of immunologic, osteogenic, and neurologic functions. *Immunologic Research*, *50*(1), 22–38.

Li, Z.-Y., Possin, D. E., & Milam, A. H. (1995). Histopathology of Bone Spicule Pigmentation in Retinitis Pigmentosa. *Ophthalmology*, *102*(5), 805–816.

Man-Kyo Chung, Ali, D. G., & Michael, J. C. (2008). TRPV1 shows dynamic ionic selectivity during agonist stimulation. *Nature Neuroscience*, *11*(5), 555.

Marc, R. E., Jones, B. W., Watt, C. B., & Strettoi, E. (2003). Neural remodeling in retinal degeneration. *Progress in Retinal and Eye Research*, *22*(5), 607–655.

Margolis, D., Newkirk, G., Euler, T., & Detwiler, P. (2008). Functional stability of retinal ganglion cells after degeneration-induced changes in synaptic input. *Journal of Neuroscience*, *28*(25), 6526–6536.

Masland, R. H. (2001). The fundamental plan of the retina. *Nature Neuroscience*, *4*(9), 877.

Mayer, M., & Westbrook, G. (1987). Permeation and block of N-methyl-D-aspartic acid receptor channels by divalent cations in mouse cultured central neurones. *Journal of Physiology (London)*, *394*(1), 501–527.

McLennan, H. (1983). Receptors for the excitatory amino acids in the mammalian central nervous system. *Progress in Neurobiology*, *20*(3–4), 251–271.

Milam, A. H., Li, Z. Y., & Fariss, R. N. (1998). Histopathology of the human retina in retinitis pigmentosa. *Progress in Retinal and Eye Research*, *17*(2), 175–205.

Nelson, R., Famiglietti, E. V., & Kolb, H. (1978). Intracellular staining reveals different levels of stratification for on- and off- center ganglion cells in cat retina. *Journal of Neurophysiology*, *41*(2), 472–483.

Neumann, E., Schaefer-Ridder, M., Wang, Y., & Hofschneider, P. H. (1982). Gene transfer into mouse lyoma cells by electroporation in high electric fields. *The EMBO Journal*, *1*(7), 841.

North, R. A. (2002). Molecular physiology of P2X receptors. *Physiological Reviews*, *82*(4), 1013–1067.

Notomi, S., Hisatomi, T., Kanemaru, T., Takeda, A., Ikeda, Y., Enaida, H., Kroemer, G., & Ishibashi, T. (2011). Critical involvement of extracellular ATP acting on P2RX7 purinergic receptors in photoreceptor cell death. *The American Journal of Pathology*, *179*(6), 2798–2809.

Ohshima, Y., Tsukimoto, M., Takenouchi, T., Harada, H., Suzuki, A., Sato, M., Kitani, H., & Kojima, S. (2010). γ- Irradiation induces P2X 7 receptor- dependent ATP release from B16 melanoma cells. *BBA - General Subjects*, *1800*(1), 40–46.

Orrenius, S., & Nicotera, P. (1994). The calcium ion and cell death. *Journal of Neural Transmission. Supplementum*, *43*, 1–11.

Palczewski, K. (2006). G protein-coupled receptor rhodopsin. *Annual Review of Biochemistry*, *75*(1), 743–767.

Pang, J.-J., Gao, F., & Wu, S. M. (2002). Relative contributions of bipolar cell and amacrine cell inputs to light responses of ON, OFF and ON– OFF retinal ganglion cells. *Vision Research*, *42*(1), 19–27.

Pannicke, T., Fischer, W., Biedermann, B., Schädlich, H., Grosche, J., Faude, F., Wiedemann, P., Allgaier, C., Illes, P., Burnstock, G., & Reichenbach, A. (2000). P2X7 receptors in Müller glial cells from the human retina. *The Journal of Neuroscience : The Official Journal of the Society for Neuroscience*, *20*(16), 5965–5972.

Pellegatti, P., Falzoni, S., Donvito, G., Lemaire, I., & Di Virgilio, F. (2011). P2X7 receptor drives osteoclast fusion by increasing the extracellular adenosine concentration. *The FASEB Journal*, *25*(4), 1264–1274.

Perez De Sevilla Müller, L., Shelley, J., & Weiler, R. (2007). Displaced amacrine cells of the mouse retina. *Journal of Comparative Neurology*, *505*(2), 177–189.

Puthussery, T., & Fletcher, E. (2009). Extracellular ATP induces retinal photoreceptor apoptosis through activation of purinoceptors in rodents. *Journal of Comparative Neurology*, *513*(4), 430–440.

Puthussery, T., Yee, P., Vingrys, A. J., & Fletcher, E. L. (2006). Evidence for the involvement of purinergic P2X7 receptors in outer retinal processing. *European Journal of Neuroscience*, *24*(1), 7–19.

Ralevic, V., & Burnstock, G. (1998). Receptors for purines and pyrimidines. *Pharmacological Reviews*, *50*(3), 413–492.

Rassendren, F., Buell, G. N., Virginio, C., Collo, G., North, R. A., & Surprenant, A. (1997). The permeabilizing ATP receptor, P2X7. cloning and expression of a human cDNA. *The Journal of Biological Chemistry*, *272*(9), 5482–5486.

Rattner, A., Sun, H., & Nathans, J. (1999). Molecular genetics of human retinal disease. *Annual Review of Genetics*, *33*, 89–131.

Remington, L. A. (2012). *Clinical anatomy and physiology of the visual system* (3rd ed..). St. Louis : Elsevier/Butterworth-Heinemann.

Retinitis Pigmentosa. (n.d.). *Fighting Blindness Canada (FBC)*. Retrieved April 9, 2020, from https://www.fightingblindness.ca/eye-diseases-pathways/retinitis-pigmentosa/

Rodriguez, A. R., Sevilla Müller, L. P., & Brecha, N. C. (2014). The RNA binding protein RBPMS is a selective marker of ganglion cells in the mammalian retina. *Journal of Comparative Neurology*, *522*(6), 1411–1443.

Saha, S., Greferath, U., Vessey, K. A., Grayden, D. B., Burkitt, A. N., & Fletcher, E. L. (2016). Changes in ganglion cells during retinal degeneration. *Neuroscience*, *329*(Journal Article), 1–11.

Sanes, J. R., & Zipursky, S. L. (2010). Design principles of insect and vertebrate visual systems. *Neuron*, *66*(1), 15–36.

Sappington, R. M., Sidorova, T., Long, D. J., & Calkins, D. J. (2009). TRPV1: contribution to retinal ganglion cell apoptosis and increased intracellular Ca^{2+} with exposure to hydrostatic pressure. *Investigative Ophthalmology & Visual Science*, *50*(2), 717–728.

Schäfer, B. W., & Heizmann, C. W. (1996). The S100 family of EF-hand calcium-binding proteins: functions and pathology. *Trends in Biochemical Sciences*, *21*(4), 134–140.

Schilling, W., Sinkins, W., & Estacion, M. (1999). Maitotoxin activates a nonselective cation channel and a P2Z/ P2X7- like cytolytic pore in human skin fibroblasts. *American Journal of Physiology*, *46*(4), C755–C765.

Schwaller, B., Meyer, M., & Schiffmann, S. (2002). `New functions for `old proteins: The role of the calcium-binding proteins calbindin D-28k, calretinin and parvalbumin, in cerebellar physiology. Studies with knockout mice. *Cerebellum*, *1*(4), 241–258.

Schwartz, S. D., Regillo, C. D., Lam, B. L., Eliott, D., Rosenfeld, P. J., Gregori, N. Z., Hubschman, J.-P., Davis, J. L., Heilwell, G., Spirn, M., Maguire, J., Gay, R., Bateman, J., Ostrick, R. M., Morris, D., Vincent, M., Anglade, E., Del Priore, L., V., & Lanza, R. (2015). Human embryonic stem cell- derived retinal pigment epithelium in patients with age- related macular degeneration and Stargardt's macular dystrophy: Follow-up of two open-label phase 1/2 studies. *The Lancet*, *385*(9967), 509–516.

Sekaran, S., Foster, R. G., Lucas, R. J., & Hankins, M. W. (2003). Calcium imaging reveals a network of intrinsically light-sensitive inner-retinal neurons. *Current Biology*, *13*(15), 1290–1298.

Silverman, J., Powers, J., Stromberg, P., Pultz, J. A., & Kent, S. (1989). Effects on C3H mouse mammary cancer of changing from a high fat to a low fat diet before, at, or after puberty. *Cancer Research*, *49*(14), 3857.

Stasheff, S. F. (2008). Emergence of sustained spontaneous hyperactivity and temporary preservation of OFF responses in ganglion cells of the retinal degeneration (rd1) mouse. *Journal of Neurophysiology*, *99*(3), 1408.

Steinberg, T., Newman, A., Swanson, J., & Silverstein, S. (1987). ATP^{4-} permeabilizes the plasma membrane of mouse macrophages to fluorescent dyes. *Journal of Biological Chemistry*, *262*(18), 8884–8895.

Strauss, O. (2005). The retinal pigment epithelium in visual function. *Physiological Reviews*, *85*(3), 845–881.

Strong, L. C. (1935, reprinted 1979). The establishment of the C3H inbred strain of mice for the study of spontaneous carcinoma of the mammary gland. *CA: A Cancer Journal for Clinicians*, *29*(1), 57–62.

Stryer, L. (1986). Cyclic GMP cascade of vision. *Annual Review of Neuroscience*, *9*(1), 87–119.

Suadicani, S., Brosnan, C., & Scemes, E. (2006). $P2X_7$ receptors mediate ATP release and amplification of astrocytic intercellular Ca^{2+} signaling. *Journal of Neuroscience*, *26*(5), 1378–1385.

Surprenant, A., Rassendren, F., Kawashima, E., North, R. A., & Buell, G. (1996). The cytolytic P2Z receptor for extracellular ATP identified as a P2X7 receptor. *Science*, *272*(5262), 735–738.

Thompson, R. J., Jackson, M. F., Olah, M. E., Rungta, R. L., Hines, D. J., Beazely, M. A., Macdonald, J. F., & Macvicar, B. A. (2008). Activation of pannexin-1 hemichannels augments aberrant bursting in the hippocampus. *Science (New York, N.Y.)*, *322*(5907), 1555–1559.

Tochitsky, I., Helft, Z., Meseguer, V., Fletcher, R. b, Vessey, K. a, Telias, M., Denlinger, B., Malis, J., Fletcher, E. l, & Kramer, R. h. (2016). How azobenzene photoswitches restore visual responses to the blind retina. *Neuron*, *92*(1), 100–113.

Tochitsky, I., Polosukhina, A., Degtyar, V. E., Gallerani, N., Smith, C. M., Friedman, A., Van Gelder, R., N., Trauner, D., Kaufer, D., & Kramer, R. H. (2014). Restoring visual function to blind mice with a photoswitch that exploits electrophysiological remodeling of retinal ganglion cells. *Neuron*, *81*(4), 800–813.

Tsien, R. Y. (1981). A non-disruptive technique for loading calcium buffers and indicators into cells. *Nature*, *290*(5806), 527.

Tsien, R. Y. (1989). Fluorescent probes of cell signaling. *Annual Review of Neuroscience*, *12*(Journal Article), 227.

Van Essen, D. C., Anderson, C. H., & Felleman, D. J. (1992). Information processing in the primate visual system: an integrated systems perspective. *Science (New York, N.Y.)*, *255*(5043), 419–423.

Virginio, C., Mackenzie, A., North, R. A., & Surprenant, A. (1999). Kinetics of cell lysis, dye uptake and permeability changes in cells expressing the rat P2X7 receptor. *The Journal of Physiology*, *519 Pt 2*(Journal Article), 335.

Virginio, C., Mackenzie, A., Rassendren, F. A., North, R. A., & Surprenant, A. (1999). Pore dilation of neuronal P2X receptor channels. *Nature Neuroscience*, *2*(4), 315.

Wässle, H., Peichl, L., Airaksinen, M. S., & Meyer, M. (1998). Calcium-binding proteins in the retina of a calbindin-null mutant mouse. *Cell and Tissue Research*, *292*(2), 211–218.

Wheeler-Schilling, T., Marquordt, K., Kohler, K., Guenther, E., & Jabs, R. (2001). Identification of purinergic receptors in retinal ganglion cells. *Molecular Brain Research*, *92*(1–2), 177–180.

Yan, Z., Li, S., Liang, Z., Tomić, M., & Stojilkovic, S. S. (2008). The P2X 7 receptor channel pore dilates under physiological ion conditions. *The Journal of General Physiology*, *132*(5), 563–573.

Yu, J., Daniels, B. A., & Baldridge, W. H. (2009). Slow excitation of cultured rat retinal ganglion cells by activating group I metabotropic glutamate receptors. *Journal of Neurophysiology*, *102*(6), 3728–3739.

Zambon, A., Bronte, V., Di Virgilio, F., Hanau, S., Steinberg, T. H., Collavo, D., & Zanovello, P. (1994). Role of extracellular ATP in cell-mediated cytotoxicity: a study with ATP-sensitive and ATP-resistant macrophages. *Cellular Immunology*, *156*(2), 458–467.

Zhang, X., Zhang, M., Laties, A. M., & Mitchell, C. H. (2005). Stimulation of P2X7 receptors elevates Ca^{2+} and kills retinal ganglion cells. *Investigative Ophthalmology & Visual Science*, *46*(6), 2183–2191.

Zrenner, E., Bartz-Schmidt, K., Benav, H., Besch, D., Bruckmann, A., Gabel, V.-P., Gekeler, F., Greppmaier, U., Harscher, A., Kibbel, S., Koch, J., Kusnyerik, A., Peters, T., Stingl, K., Sachs, H., Stett, A., Szurman, P., Wilhelm, B., & Wilke, R. (2011). Subretinal electronic chips allow blind patients to read letters and combine them to words. *Proceedings of the Royal Society B*, *278*(1711), 1489–1497.